Multi-technique characterization of ionospheric Space Weather effects

Ashik Paul, Lucilla Alfonsi, Haris Haralambous, Sarbani Ray, Claudio Cesaroni, Christina Oikonomou, Dibyendu Sur

Institute of Radio Physics and Electronics, University of Calcutta, India
National Institute of Geophysics and Volcanology (INGV), Italy
Frederick University, Cyprus

ap.rpe@caluniv.ac.in

League of Extraordinary Scientists

➢**Prof. S. K. Mitra was one of the first in the world to suggest use of HF atmospheric radars with his observations in 1935**

Professor S.K. Mitra and Dr. A.P. Mitra
URSI General Assembly, Sydney, 1952

- **The *first experimental evidence of E layer predicted* by Heaviside and Kennely was obtained by Mitra and Rakshit in 1930.**

- **His seminal book 'The Upper Atmosphere' has been considered a Bible for researchers in the field.**

This Department was the First in India to start Post-Graduate teaching in Electronics

- The Ionosphere Field Station was established in 1953 at Haringhata, about 50km north-east of Calcutta at a place of relatively low radio frequency interference.

- Professor Mitra assembled the **First manual Ionospheric Sounding System** in Asia in *1954* and established it at the *Ionospheric Field Station in 1956* thereby putting University of Calcutta in an elite global chain of Ionospheric Sounders.

- **NBS-C2 Ionosonde data** for the period 1957-1976 from *Ionosphere Field Station* at Haringhata available at the **Space Physics Interactive Data Resources (SPIDR)** website under the ***National Geophysical Data Center located at Boulder, Colorado, USA***

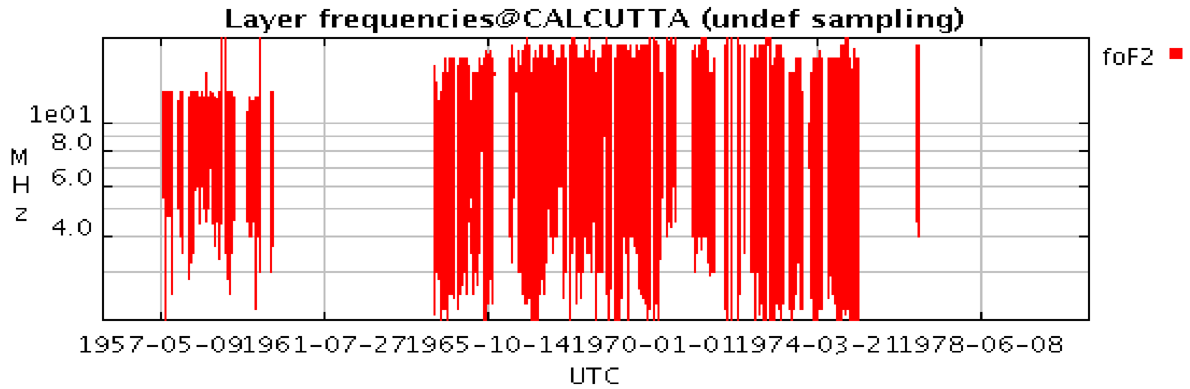

SPACE SITUATIONAL AWARENESS

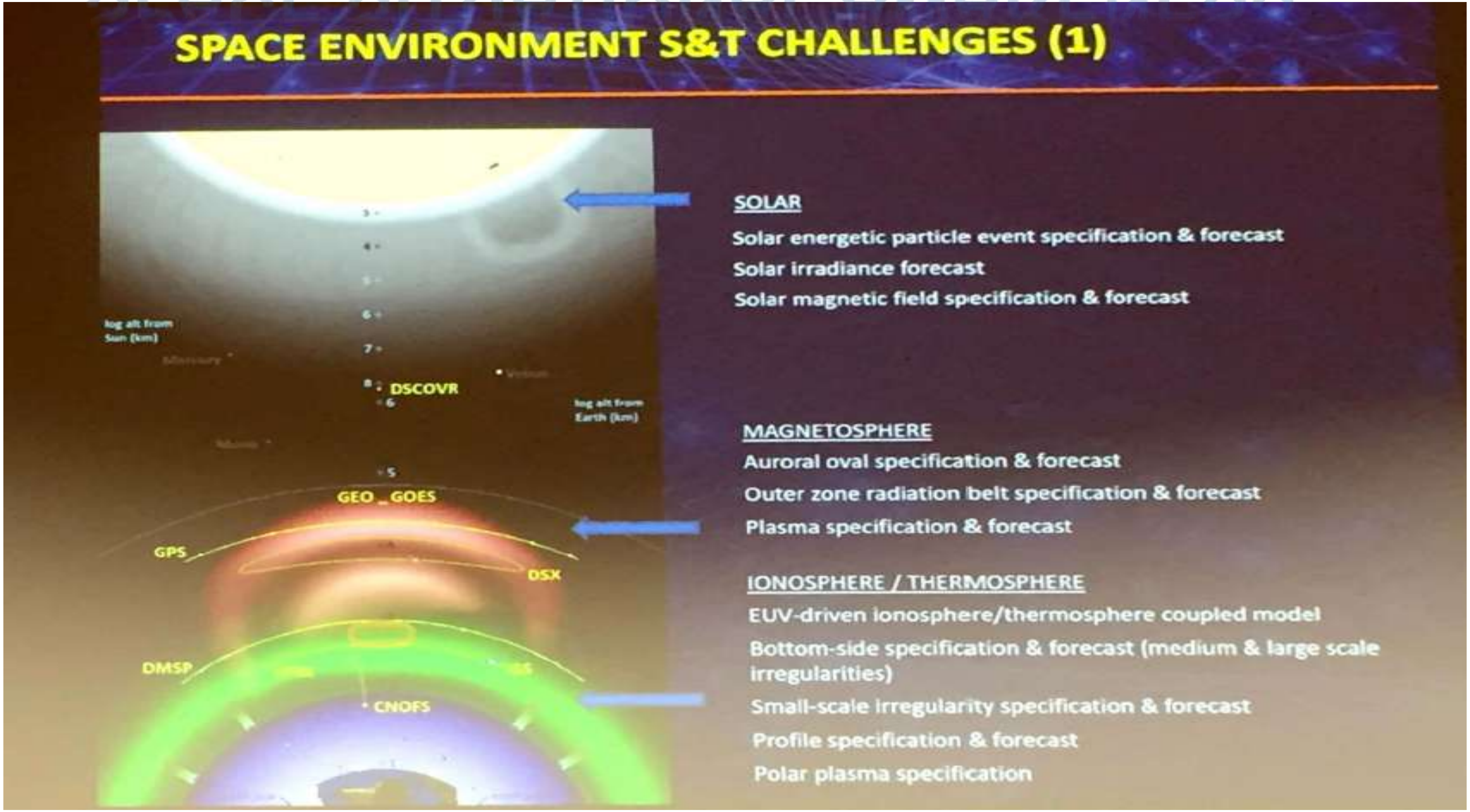

Near Earth Space Environment

Geostationary Neighbourhood

The orbit plane of a GEO satellite which ceases inclination control will evolve to a maximum inclination of 15° after 27 years and then return to the GEO belt after 53 years (nearly 55 years for 600km above GEO. This is caused by solar and lunar gravitational perturbations on the orbit plane.

Plot shows the inclination vectors of near GEO objects from Space-Track Catalogue as of July 2017.
Satellites which stopped inclination control are starting to return to the GEO belt (credit Oltrogge AGI 2017)

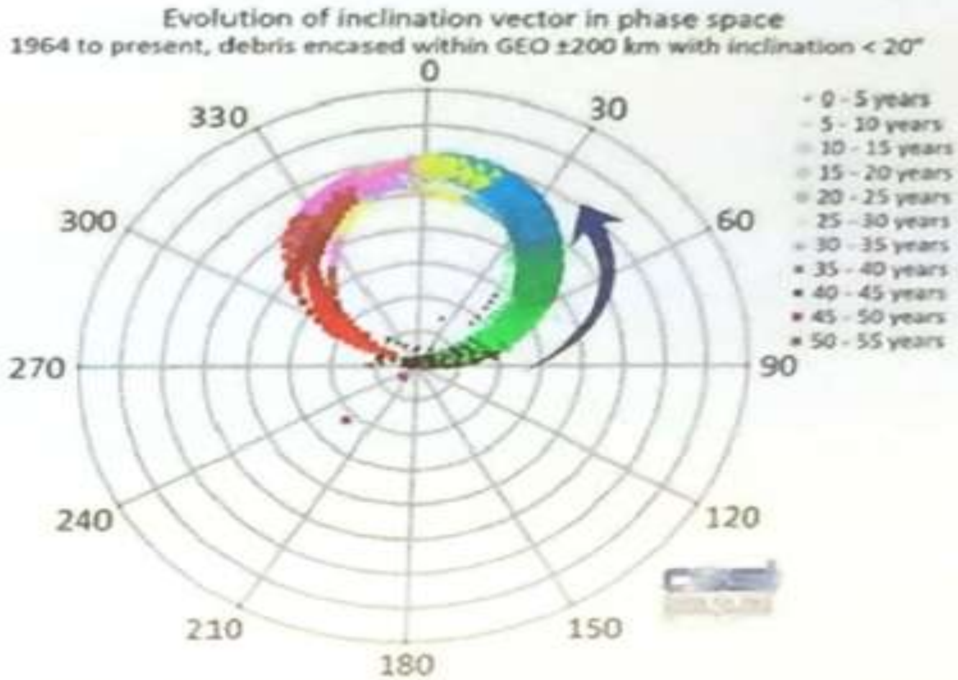

Over the next decade 2020-2030 GEO satellites which were deorbited /abandoned in 1966-1976 will start to return to the GEO belt altering the makeup of the GEO debris population

The relative encounter velocities between controlled GEO satellites and uncontrolled satellites originating from GEO can be as high as 800 m/s for the maximum inclination of 15°.

- **Space systems and services operate in and through the natural space environment, so to have complete space situational awareness, we need to understand the natural space environment, for example:**
  - Solar particle and electromagnetic radiation
  - Interplanetary phenomenon--e.g. CMEs, Coronal holes
  - Magnetospheric radiation, fields, and currents
  - Upper atmospheric density, temperature and winds
  - Ionospheric density
  - Galactic cosmic radiation
  - Meteors
- **We need to understand the environment's effects on space systems and services**

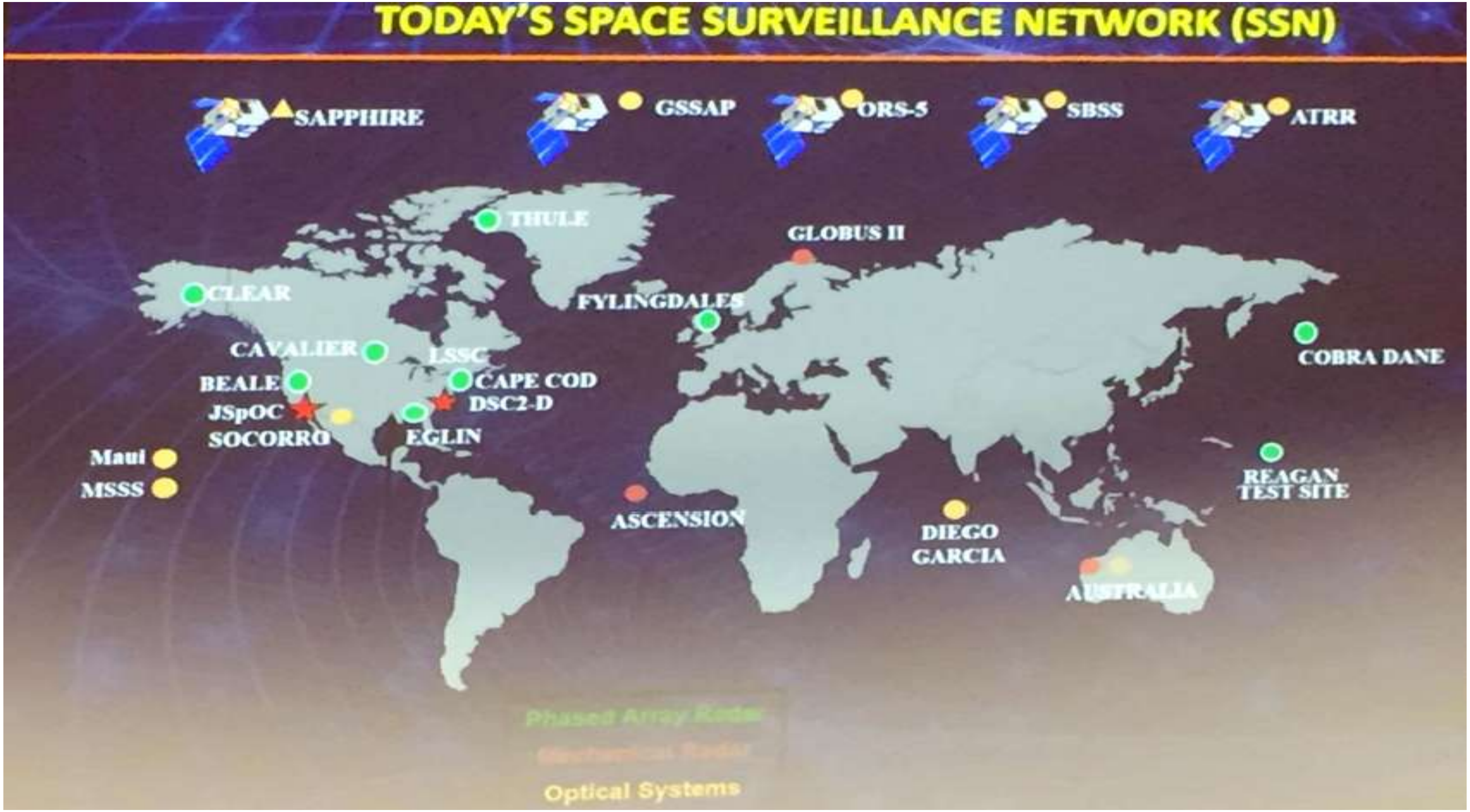
TODAY'S SPACE SURVEILLANCE NETWORK (SSN)
SAPPHIRE
GSSAP
ORS-5
SBSS
ATRR
THULE
GLOBUS II
CLEAR
FYLINGDALES
CAVALIER
LSSC
CAPE COD
BEALE
JSpOC
DSC2-D
SOCORRO
EGLIN
COBRA DANE
Maui
MSSS
REAGAN TEST SITE
ASCENSION
DIEGO GARCIA
AUSTRALIA
Optical Systems

SCINDA (SCIntillation Network Decision Aid) station of the US Air Force since November 2006 at the Institute of Radio Physics and Electronics, University of Calcutta, Calcutta

Global distribution of SCINDA stations

DTU

UNIVERSITY OF BATH

UiO : Universitetet i Oslo

FREDERICK UNIVERSITY CYPRUS

Istituto Nazionale di Geofisica e Vulcanologia

Multi-technique characterization of near-Earth Space Environment

Ashik Paul Lucilla Alfonsi Haris Haralambous Sarbani Ray Christina Oikonomou Claudio Cesaroni Per Hoeg Tibor Durgonics Biagio Forte Dibyendu Sur

ap.rpe@caluniv.ac.in lucilla.alfonsi@ingv.it eng.hh@fit.ac.cy
sarbanir@yahoo.com res.ec@frederick.ac.cy
claudio.cesaroni@ingv.it per.hoeg@fys.uio.no
tibdu@space.dtu.dk B.Forte@bath.ac.uk
dibyendumalay@gmail.com

INTERNATIONAL SPACE SCIENCE INSTITUTE

http://www.issibern.ch/teams/mtconese/

- Ionospheric Space Weather effects pose a major challenge to reliable GNSS based operations even after extensive research globally.

- Occurrence of spread-F, ionospheric TEC gradients and scintillations significantly perturb the performance of transionospheric satellite-based communication and navigation systems which may pose life-critical conditions, particularly for high dynamic platforms like aircrafts and adversely affect different strata of modern society.

- In terms of the intensity of ionospheric propagation effects, the polar and equatorial regions provide worst-case scenario and results obtained in these regions serve as a benchmark for the international Space Weather community.

- Interestingly, at equatorial and low latitudes, impact of ionospheric irregularities occurs even under geomagnetic benign conditions

- The scope of this work encompasses scientific inputs to advance the present understanding of Space Weather generated perturbations on technological systems.

In the present program, efforts are being made to achieve the following objectives:

1. i.) Comparison of the thermosphere-ionosphere effects of St. Patrick day storms of 2013 and 2015 over Europe, ii) effects of the geomagnetic storm of September 2017 over Europe, South-East Asia as well as Brazilian longitudes iii) effects of Joule heating and composition changes observed during intense geomagnetic storms of 2015-2017

2. Satellite signal outages observed from a network of stations distributed over low latitudes, mid latitudes and polar region within a longitude swath during periods of scintillations to check conformity with ICAO specified requirements for APV

3. Identify and characterize definitive condition for enhancement or inhibition of scintillation activities corresponding to intense geomagnetic storms. There are plans to develop long-term statistics for the low latitudes focussing on the geophysically sensitive Indian longitude sector

Comparison of the thermosphere-ionosphere effects of St. Patrick day storm of 2013 and 2015 over Europe

Geomagnetic conditions

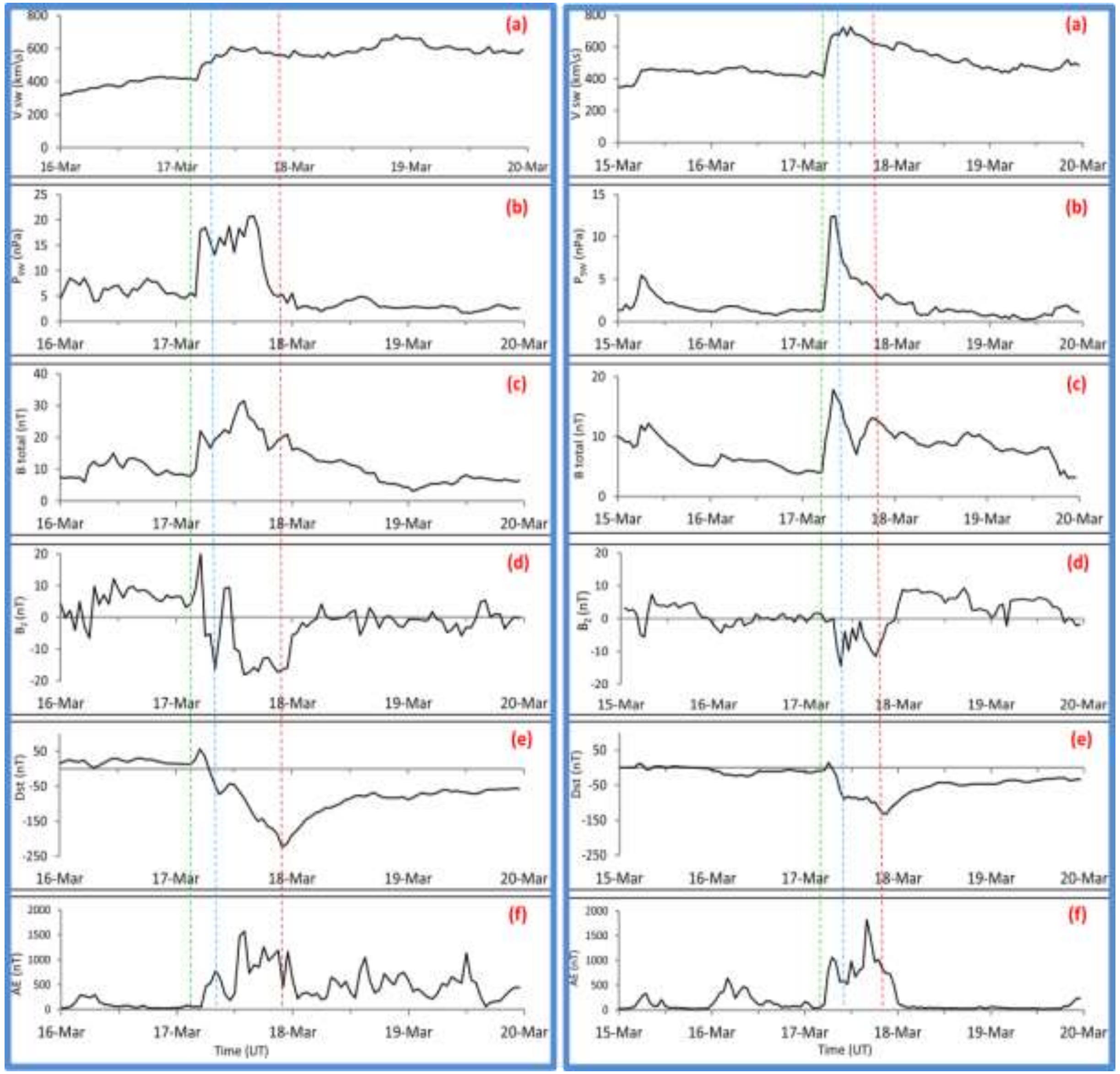

Geomagnetic conditions during the St. Patrick magnetic storms on 16–19 March 2015 (left panel) and 15–19 March 2013 (right panel). It is shown: (a) Solar wind speed, (b) Solar wind pressure, (c) total magnitude B of IMF (d) Bz component of IMF, (e) Dst ring current index, and (f) AE auroral electrojet index. The green vertical line represents the time of sudden storm commencement and the blue and red vertical lines indicate the 1st and 2nd Dst index minima respectively.

The geomagnetic storms on 17 March 2013 and 2015 present similar features though they exhibit different intensities. They were both induced by a Coronal Mass Ejection (CME) and commenced at approximately the same time (5 UT). Their main phase peaked at the same time (21-22 UT) and was marked with two minima of the Dst ring current index which occurred at almost same moments (around 10 and 22 UT).

Haralambous et al., J. Geophys. Res., 2019 (under review)

Map of GNSS receiver stations (blue) and ionosonde stations (red)

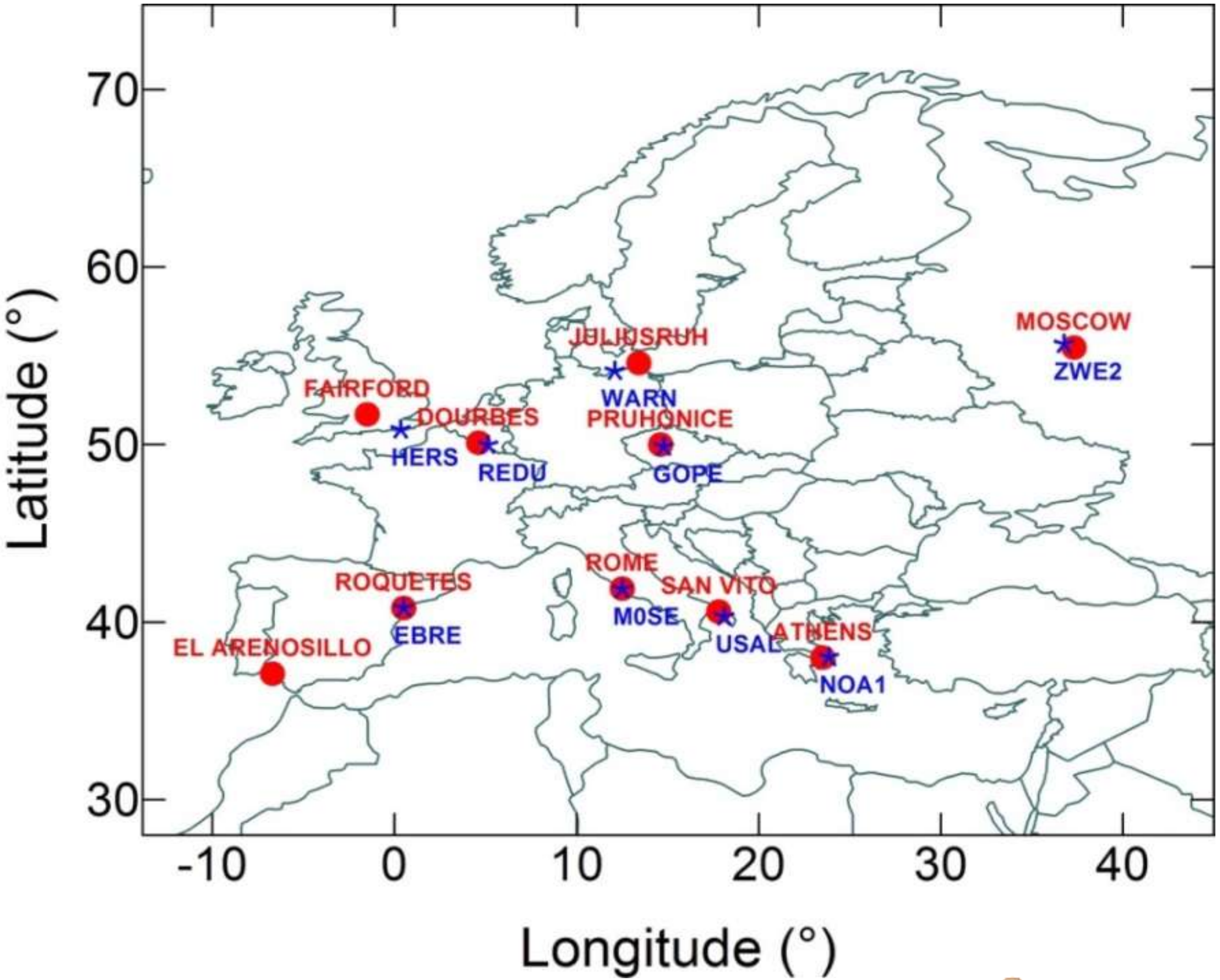

DIAS network

Haralambous et al., J. Geophys. Res., 2019 (under review)

Temporal variations of ionospheric F region characteristics

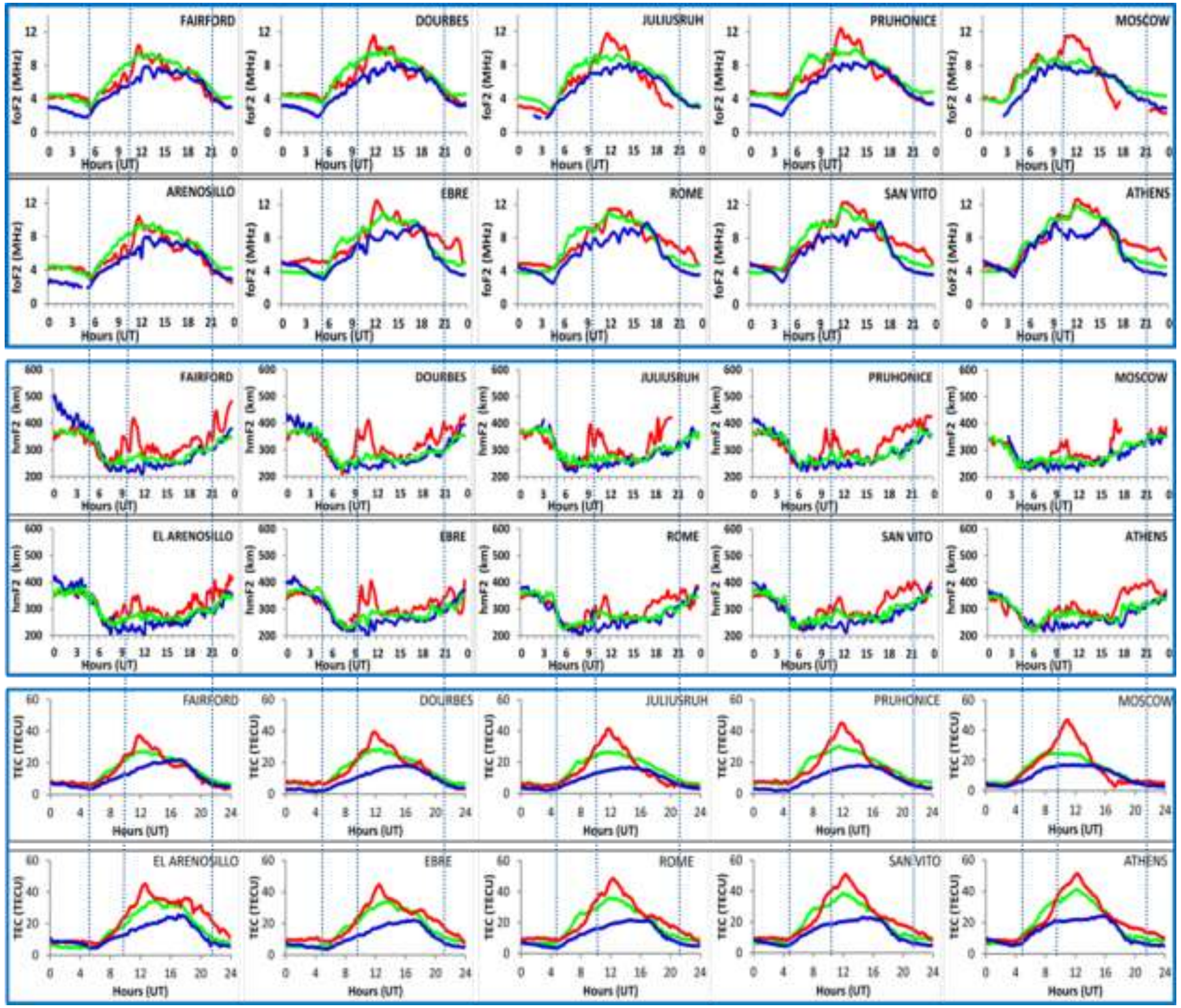

16-17 March 2013

Temporal variations of ionospheric F region characteristics foF2 (upper panel), hmF2 (middle panel) and TEC (lower panel) in Fairford, Dourbes, Juliusruh, Pruhonice, Moscow, El Arenosillo, Ebre, Rome, San Vito and Athens stations during 16-17 March 2013. Green solid lines represent the quiet reference day (16 March) and red and blue solid lines represent storm variations on 17 and 18 March respectively. Light blue vertical lines denote the sudden storm commencement time (5 UT) and the time of 1st and 2nd successive D_{st} index minima (10 and 21 UT) in 17 March 2013)

Haralambous et al., J. Geophys. Res., 2019 (under review)

Temporal variations of ionospheric F region characteristics

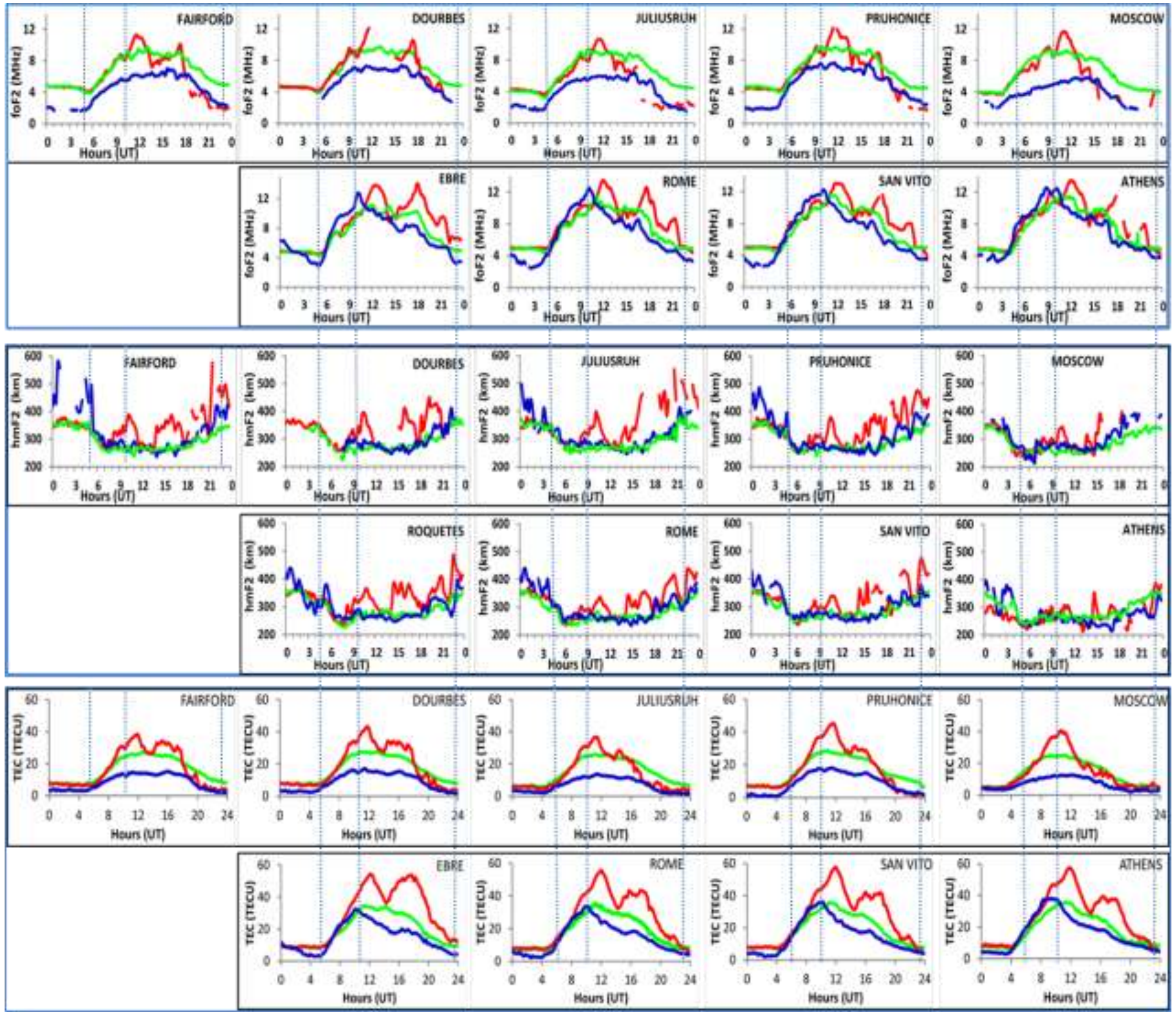

16-17 March 2015

Temporal variations of ionospheric F region characteristics foF2 (upper panel), hmF2 (middle panel) and TEC (lower panel) in Fairford, Dourbes, Juliusruh, Pruhonice, Moscow, Ebre, Rome, San Vito and Athens stations during 16-17 March 2015. Green solid lines represent the quiet reference day (16 March) and red and blue solid lines represent storm variations on 17 and 18 March respectively. Light blue vertical lines denote the sudden storm commencement time (04:45 UT) and the time of 1st and 2nd successive Dst index minima (10 UT and 22:45 UT) in 17 March 2015

Haralambous et al., J. Geophys. Res., 2019 (under review)

TEC over Europe - day to day effect

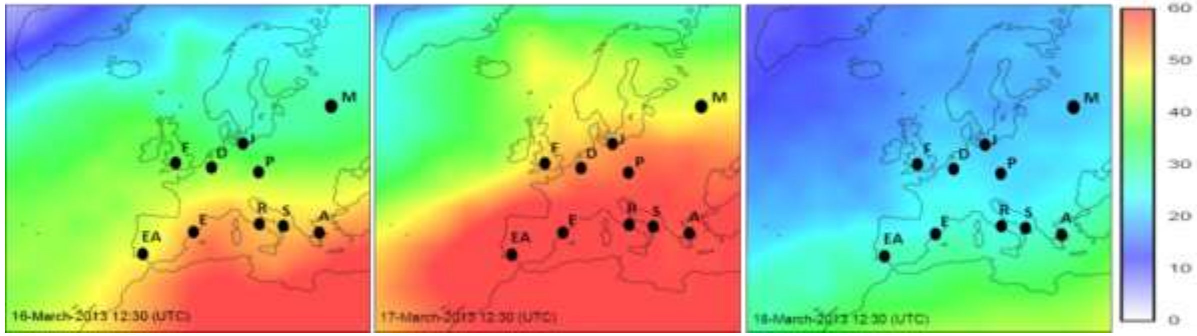

16 to 18 March 2013, 12:30 UT

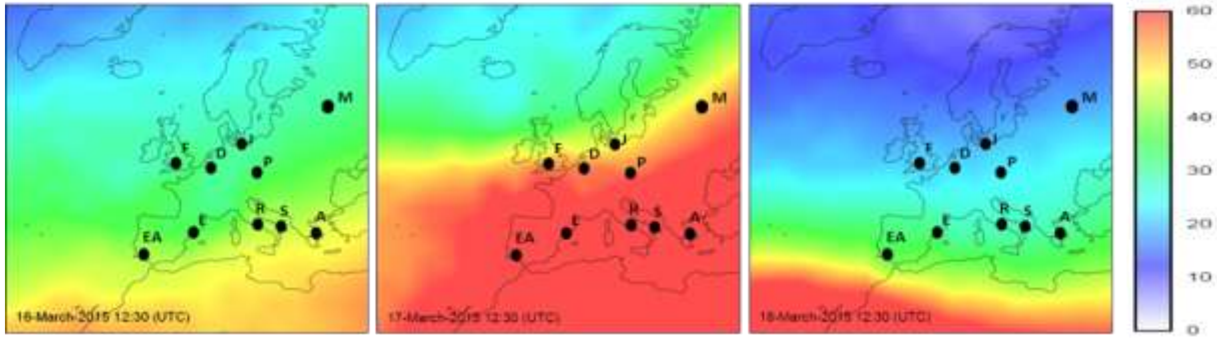

16 to 18 March 2015, 12:30 UT

INGV TEC plots confirming MIDAS maps

17 March 2013, 22UT		**17 March 2015, 23UT**	
INGV TEC plots	**MIDAS** TEC maps	**MIDAS** TEC maps	**INGV** TEC plots

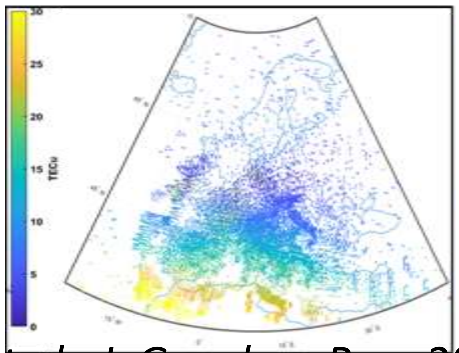

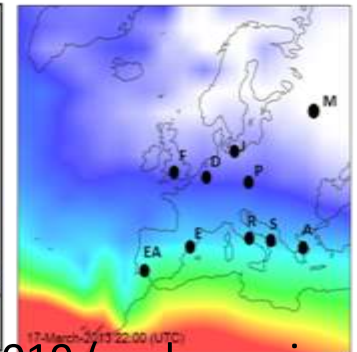

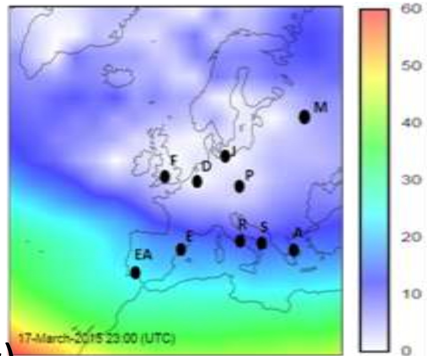

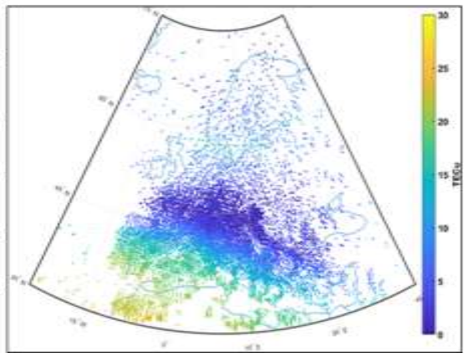

Haralambous et al., J. Geophys. Res., 2019 (under review)

TEC over Europe demonstrating TEC mid-latitude trough migration towards south

17 March 2013, 19-23 UT

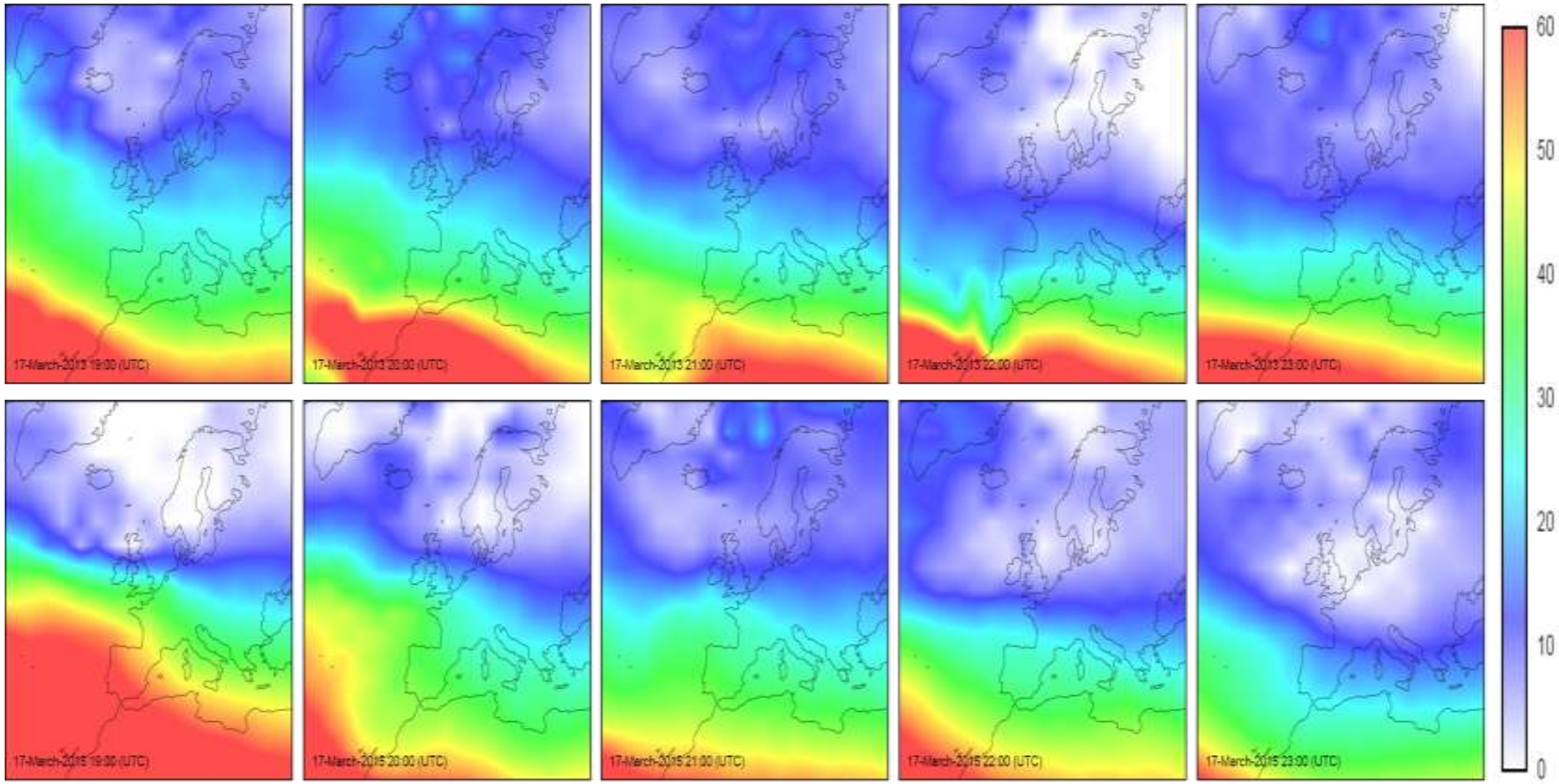

17 March 2015, 19-23 UT

Haralambous et al., *J. Geophys. Res.*, 2019 (under review)

Spread F phenomena in March 2013 storm event

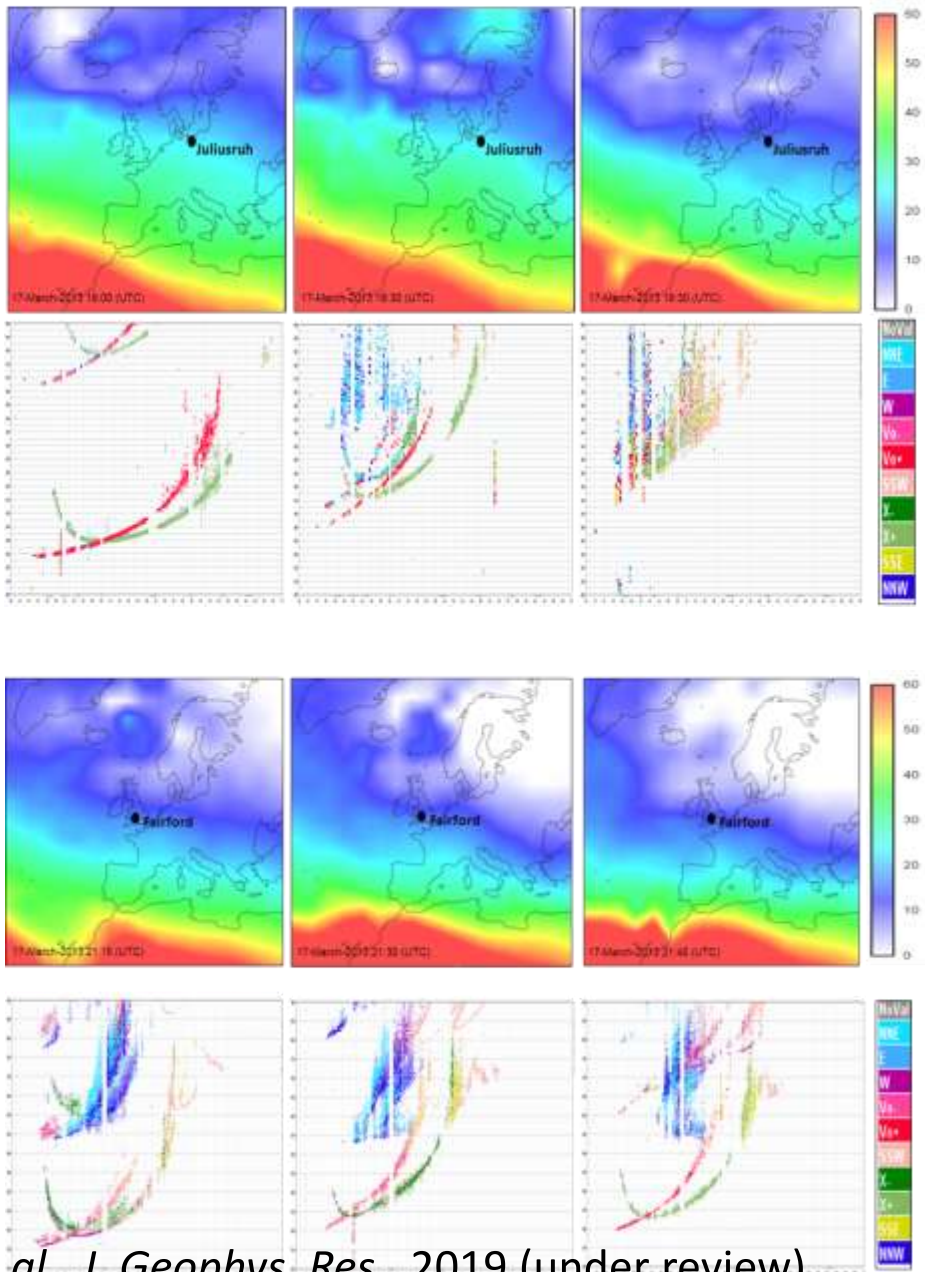

17 March 2013,
18:00 , 18:30, 19:30 UT

17 March 2013,
21:15, 21:30, 21:45 UT

Haralambous et al., J. Geophys. Res., 2019 (under review)

Spread F phenomena in March 2015 storm event

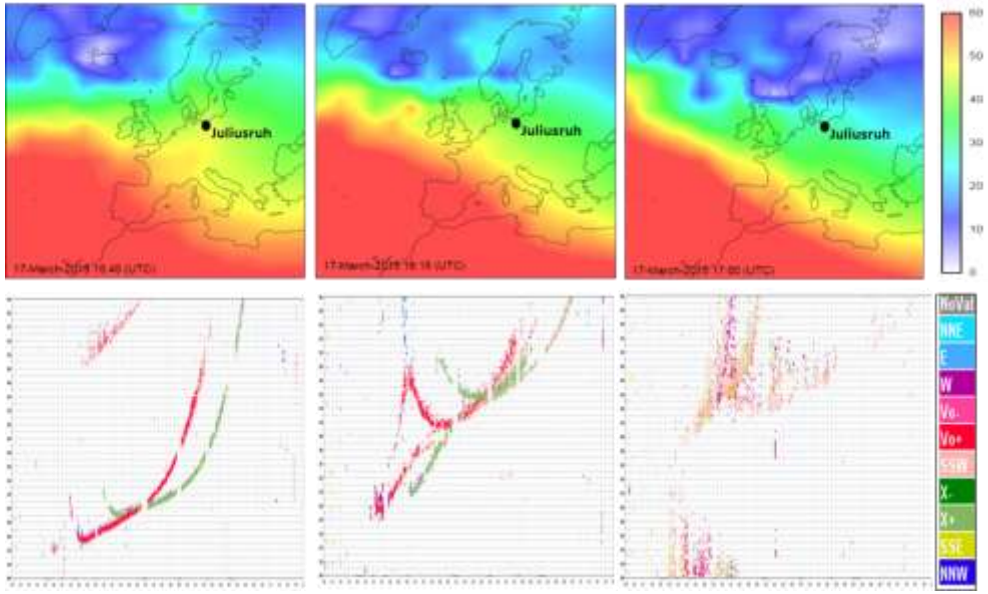

17 March 2015,
15:45 , 16:15 , 17:00
UT

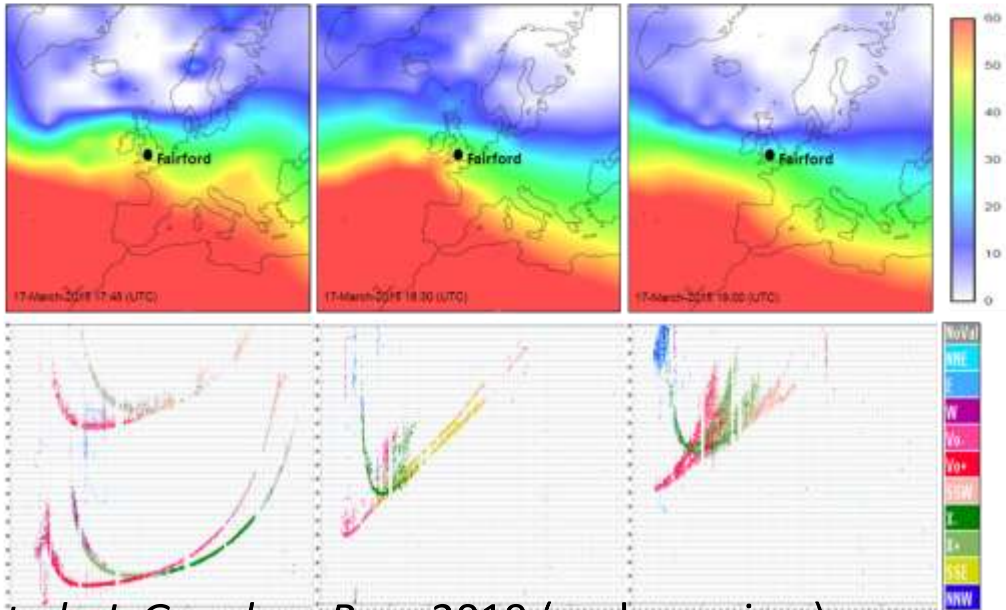

17 March 2015,
17:45, 18:30 , 19:00 UT

Haralambous et al., J. Geophys. Res., 2019 (under review)

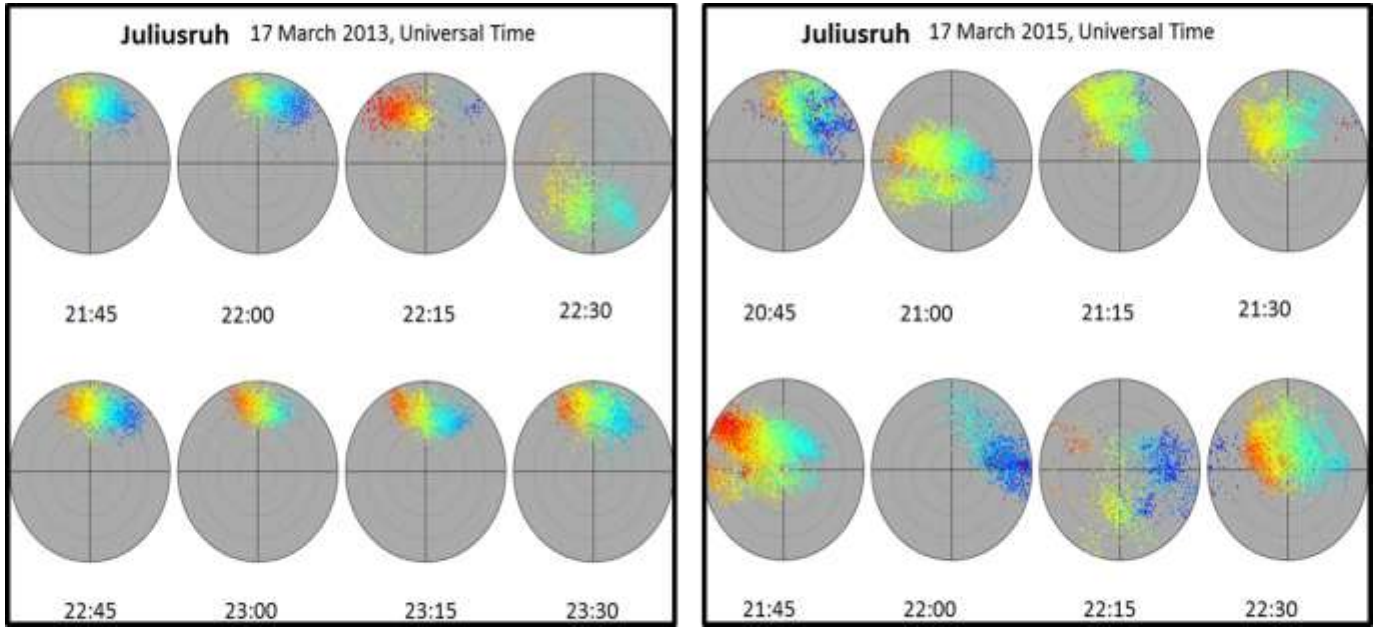

F-region 15 min skymaps recorded on a) March 17, 2013 (21:45 to 22:30 UT) in right panel, and b) March 17, 2015 (20:45 to 22:30 UT) in left panel over Juliusruh station show horizontal location of reflection points. Values of Doppler shifts are distinguished by different colors.

TID signatures propagating at low mid-latitude

Athens 17 March 2015

Vz - Vnorth - Veast (m/s)

- Quite average Vz
- Real Vz observations

Vz

Vnorth

Veast

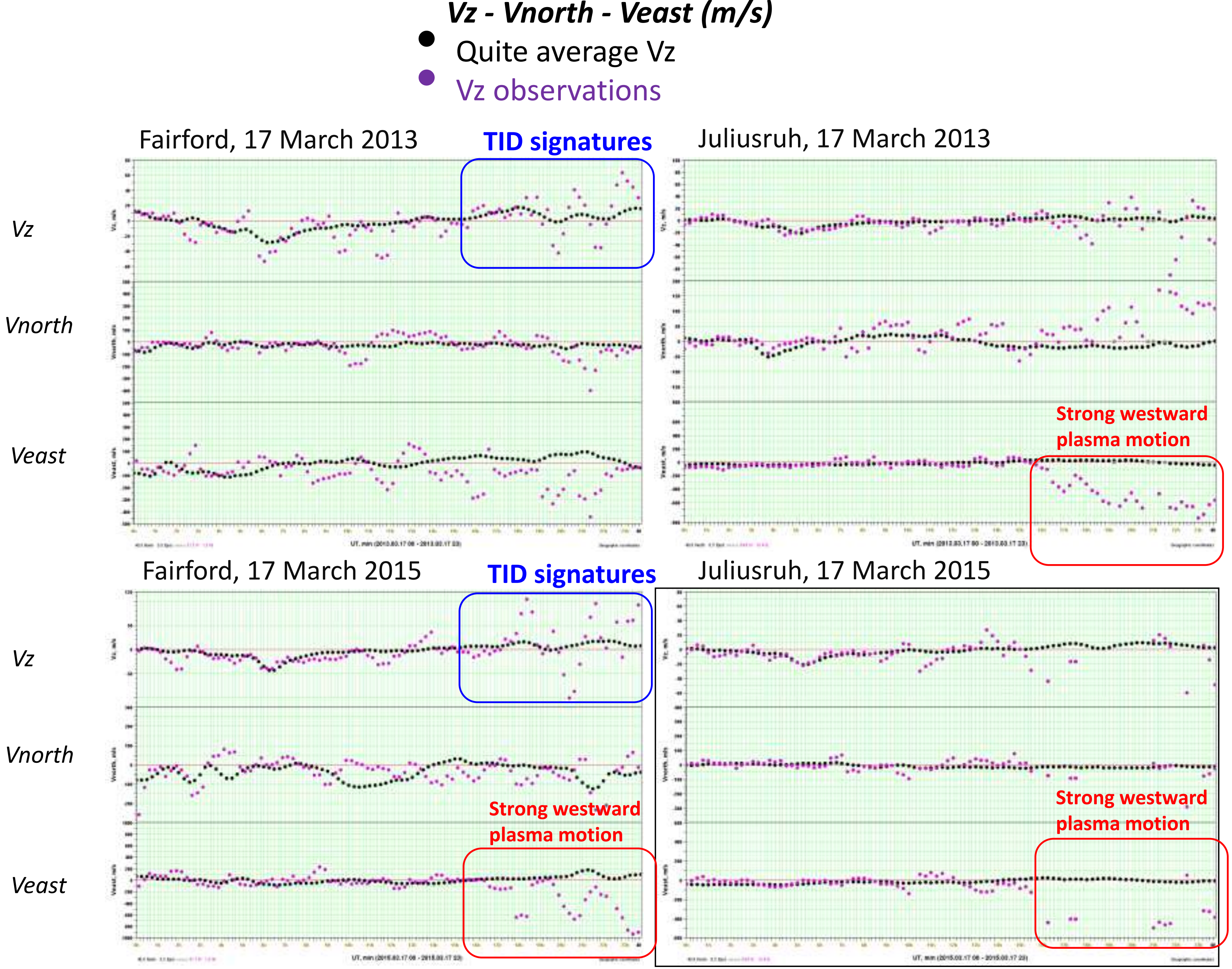

Vz - Vnorth - Veast (m/s)
Quite average Vz
Vz observations
Fairford, 17 March 2013
TID signatures
Juliusruh, 17 March 2013
Vz
Vnorth
Veast
Strong westward plasma motion
Fairford, 17 March 2015
TID signatures
Juliusruh, 17 March 2015
Vz
Vnorth
Veast
Strong westward plasma motion
Strong westward plasma motion

Effects of the geomagnetic storm of September 2017 over Europe, South-East Asia as well as Brazilian longitudes

Global ionospheric response & impact of the 7-8 September 2017 geomagnetic storm

Geomagnetic conditions

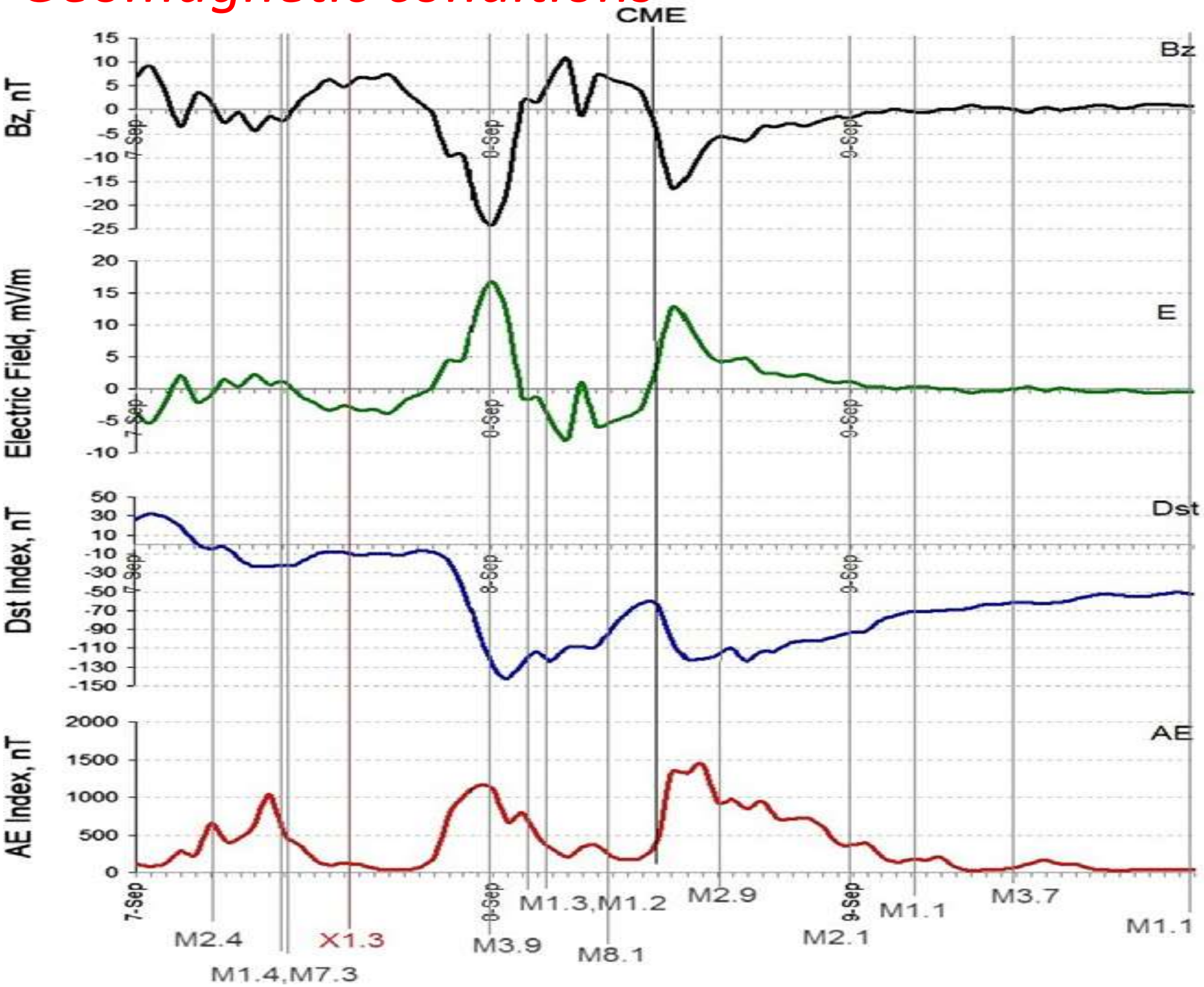

The storm event of September 7–8, 2017, is a rare event because:

a) It is not one storm with two-step main phase, but it consists of two successive storms close in time

b) Each storm was triggered not by a combination, but by independent mechanisms

c) The successive two Dst decreases had similar intensity, duration and shape of the Dst-curve.

Complex Geomagnetic conditions on Sep 7-9 2017 event

- **Solar flares- M-flare events:**

- Two intense X-flares occurred on September 6th (X2.2 at 08:57 UT and X9.3 at 11:52 UT).
- A third intense flare X1.3 at 14:20 UT on September 7th occurred some hours before the first Dst-minimum.
- Another X8.2 was detected on September 10th.
- During the considered storm event the sequence of M-flares accompanied the disturbances

- The first Dst minimum was caused by solar wind that was perturbed by the shock wave of the CME that occurred on Sep 6, but did not arrive to the Earth (not Earth directed).
- The shock wave of the next CME which was detected at Earth on Sep. 7 (22:38 UT) may have enhanced the fall of Dst to its first minimum. The CME material arrived at 11:00 UT Sep 8 at Earth causing the second Dst minimum. The first Dst minima caused by southward Bz-component of the IMF and by the consequent increases of the electric field induced into magnetosphere. Therefore, the ionosphere before the first Dst minimum was affected by flares.
- The ionosphere before and during the second Dst minimum development was affected by the previously and currently disturbed geomagnetic field and also with the preceding flares.
- **The two Dst minima were the results of two different reconnections between the Earth's magnetic field and the interplanetary magnetic field triggered by different Solar events.**

Data & Methodology

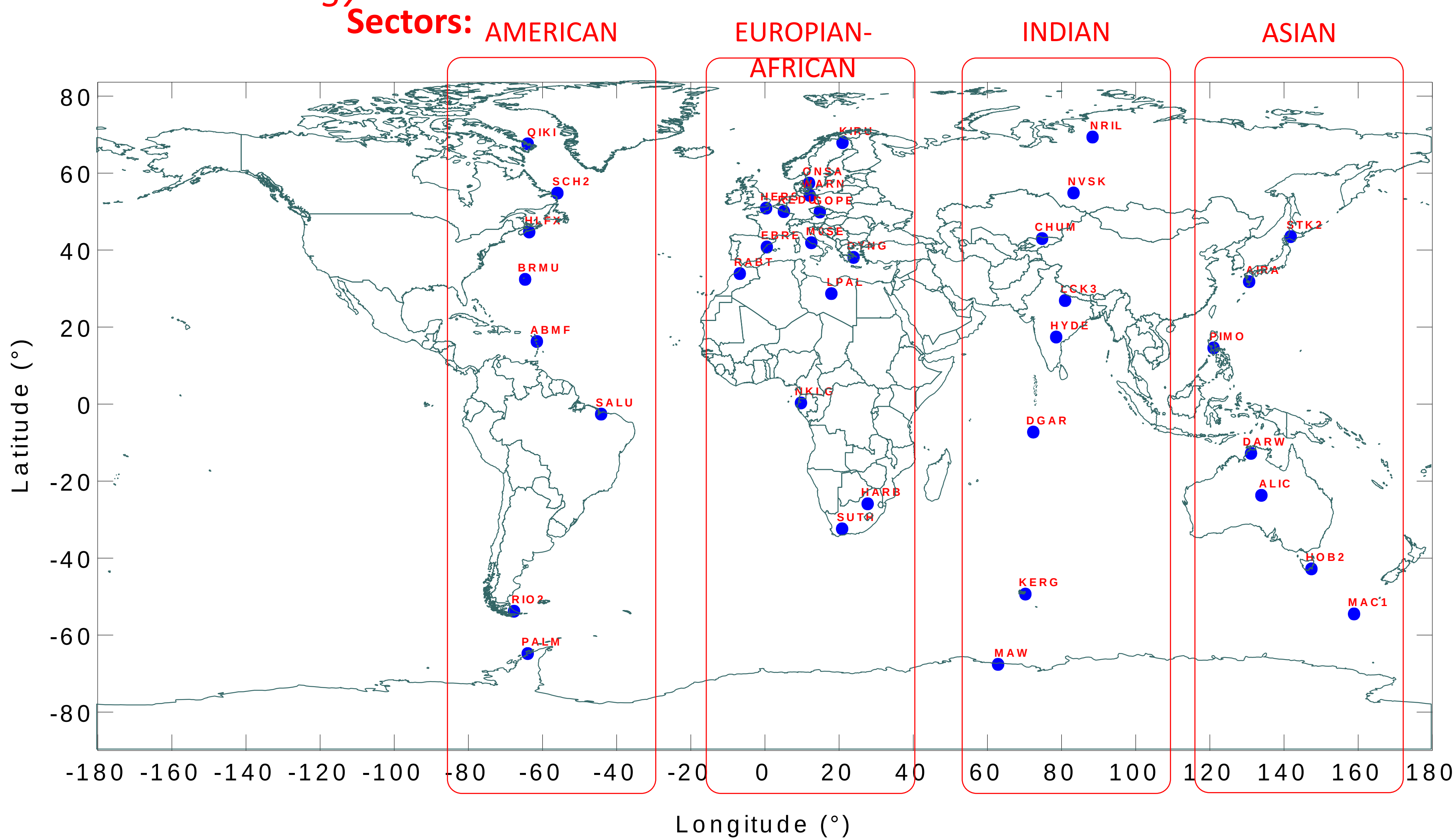

❖ We used RINEX files from GNSS permanent stations globally from:

a) International GNSS Service (IGS) http://www.igs.org/

b) EUREF Permanent Network: http://www.epncb.oma.be/index.php

❖ These files have been processed with a calibration algorithm to obtain vertical total electron content, vTEC (Ciraolo, 2012)

❖ This processing technique assumes ionospheric thin shell model (located at 350km of altitude) to obtain vTEC from slant total electron content (sTEC) at the Ionospheric Pierce Point (IPP)

Global ionospheric response to Sep 7-8, 2017 storm event

*Negative ionospheric response over **middle & high-middle latitude** areas except Asian sector*

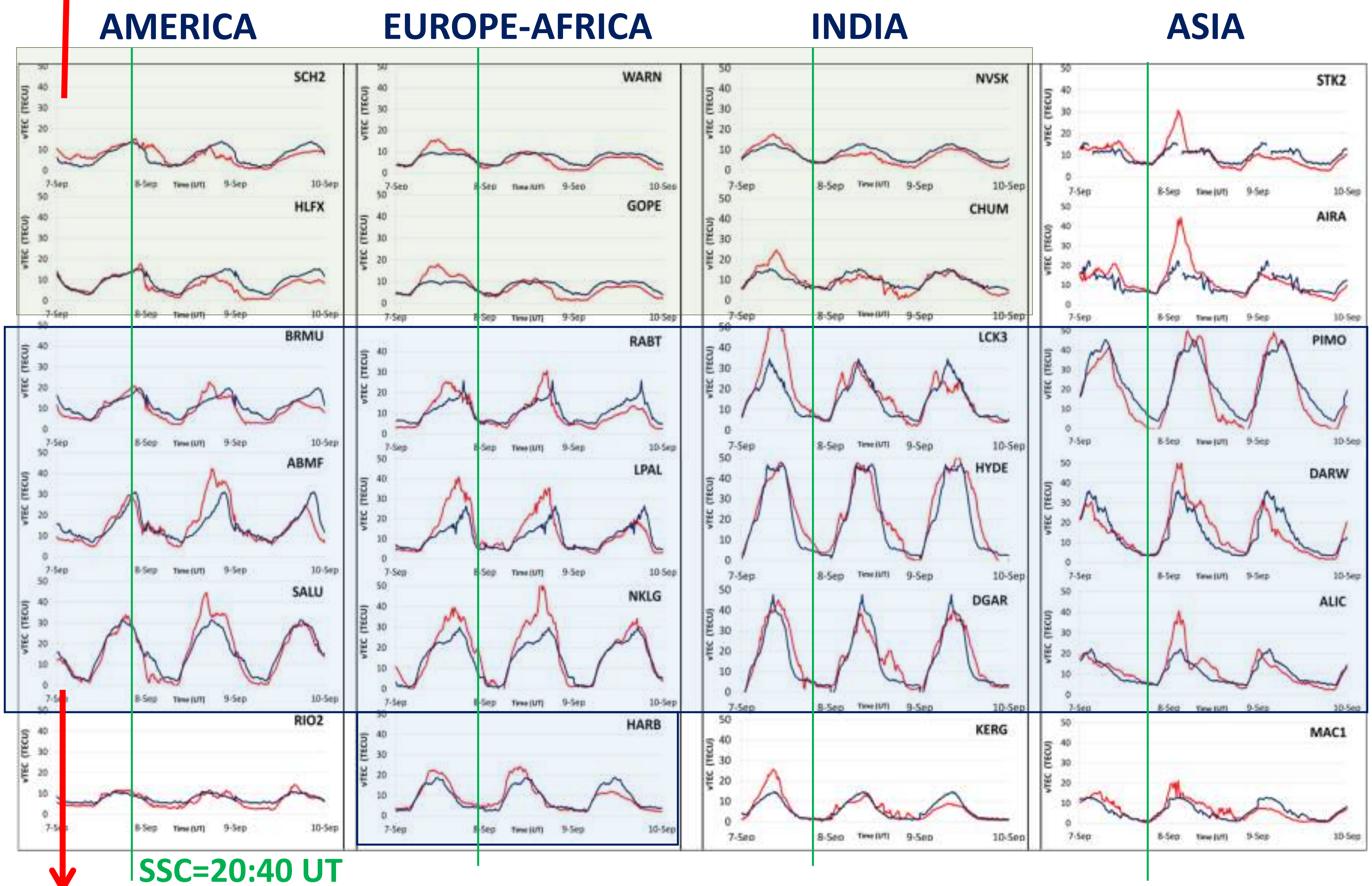

*positive ionospheric response over **equatorial-low latitude** areas in ALL 4 sectors. Not strong in India*

In general positive ionospheric response over ***equatorial-low latitude*** *areas in ALL 4 sectors*
→ Prölls classification: category 2: *Positive Storm Effects Caused by Changes in the Large-Scale Wind Circulation*

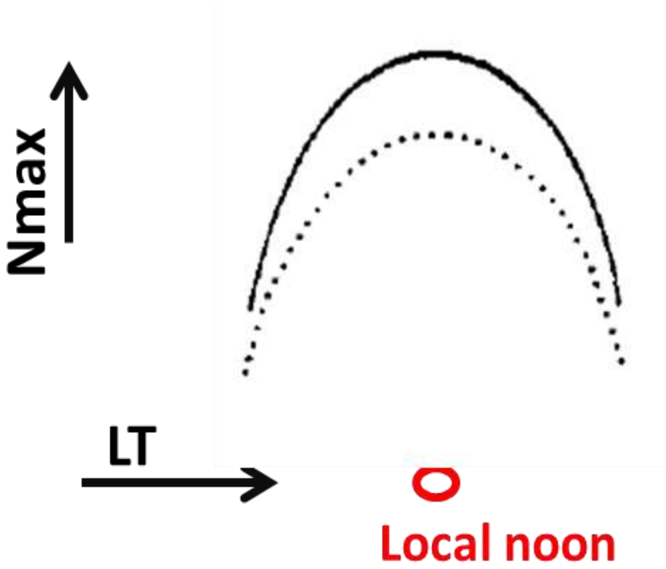

- Large spatial and temporal extent. It may last a whole day and cover the whole range of middle latitudes
- These effects are most probably caused by changes in the large-scale wind circulation
- Poleward directed winds reduced and equatorial directed winds increased
- Frequently observed in the wake of travelling positive storm effects which initiate or accompany changes in the large-scale wind circulation

Negative ionospheric response over ***middle & high-middle latitude*** *areas except Asian sector →*

→ ***Prölls classification: category 4:***

Negative Storm Effects Caused by Perturbations of the Neutral Gas Composition

FIRST STORM EVENT

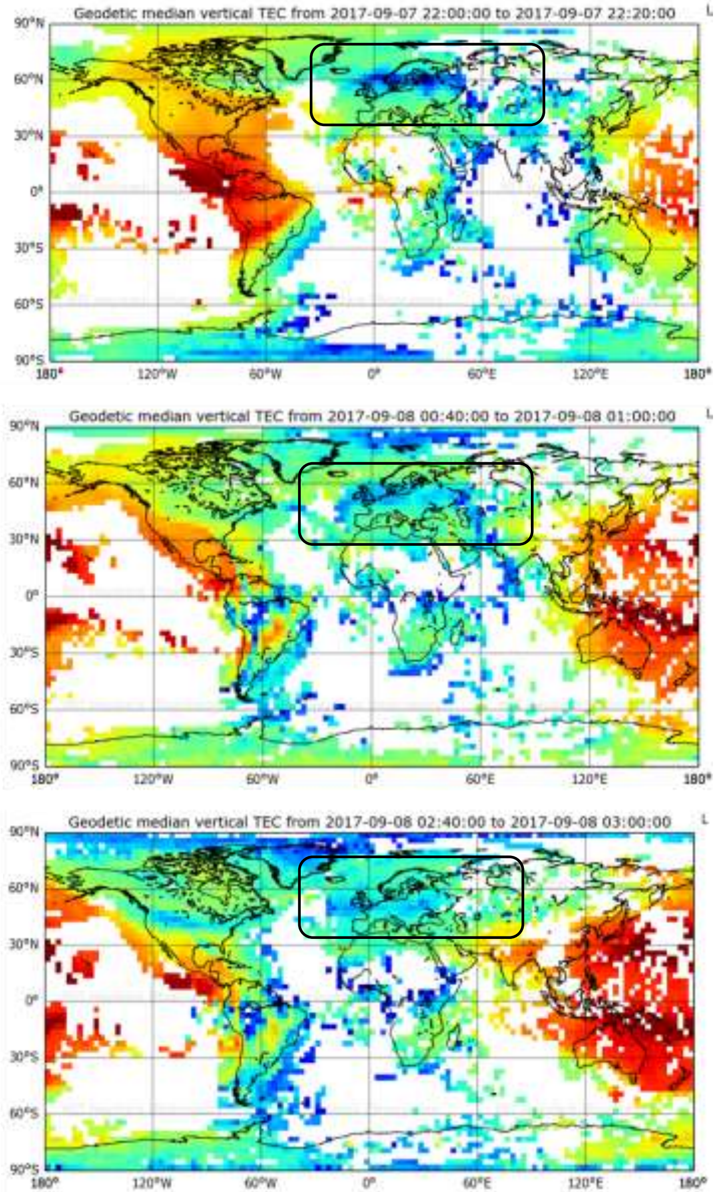

SECOND STORM EVENT

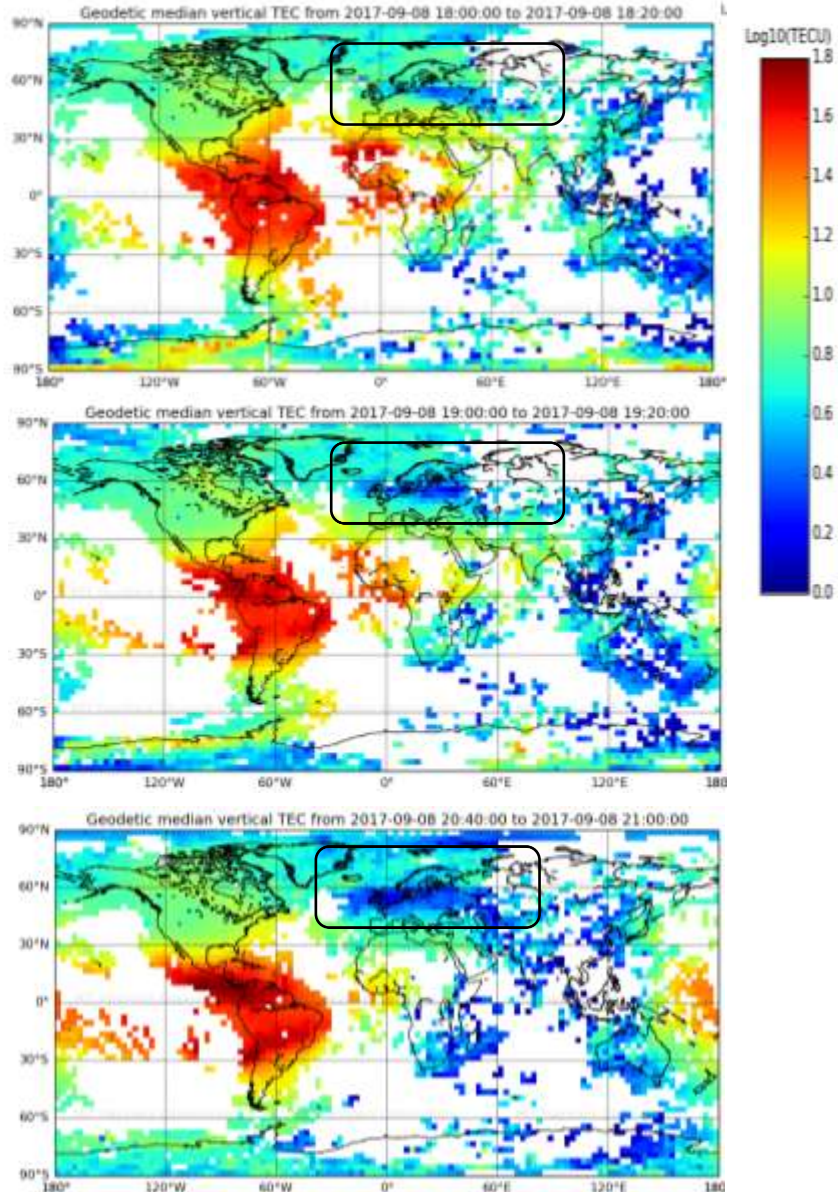

*Negative ionospheric response over **middle & high-middle latitude** areas except Asian sector →*

*→ **Prölls classification: category 4:***

Negative Storm Effects Caused by Perturbations of the Neutral Gas Composition

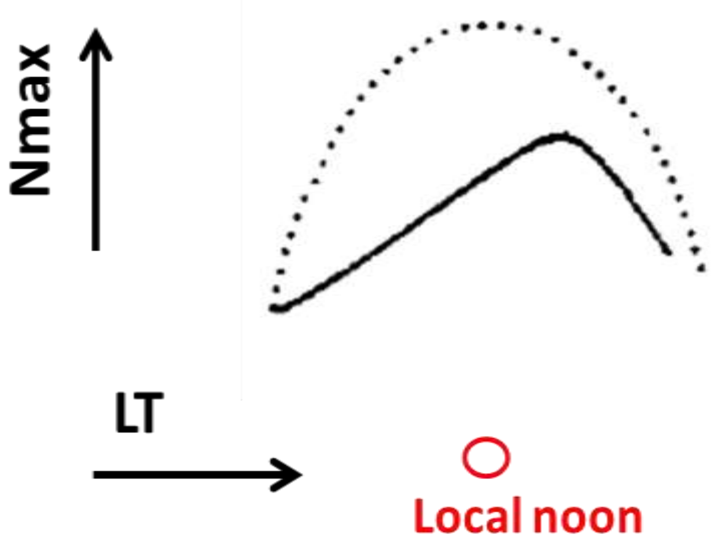

- Negative storm most clearly observed in the morning sector
- It is marked by an anomalous low rate of ionization increase after sunrise
- Its duration is of the order of many hours and may reach days during continuous magnetic activity
- Sometimes it originates from changes in the neutral gas composition
- Its onset is determined by the preferential expansion of the composition disturbance in the midnight/early morning sector and by the effectiveness of competing processes

Ionospheric effects of Sep 7-8 2017

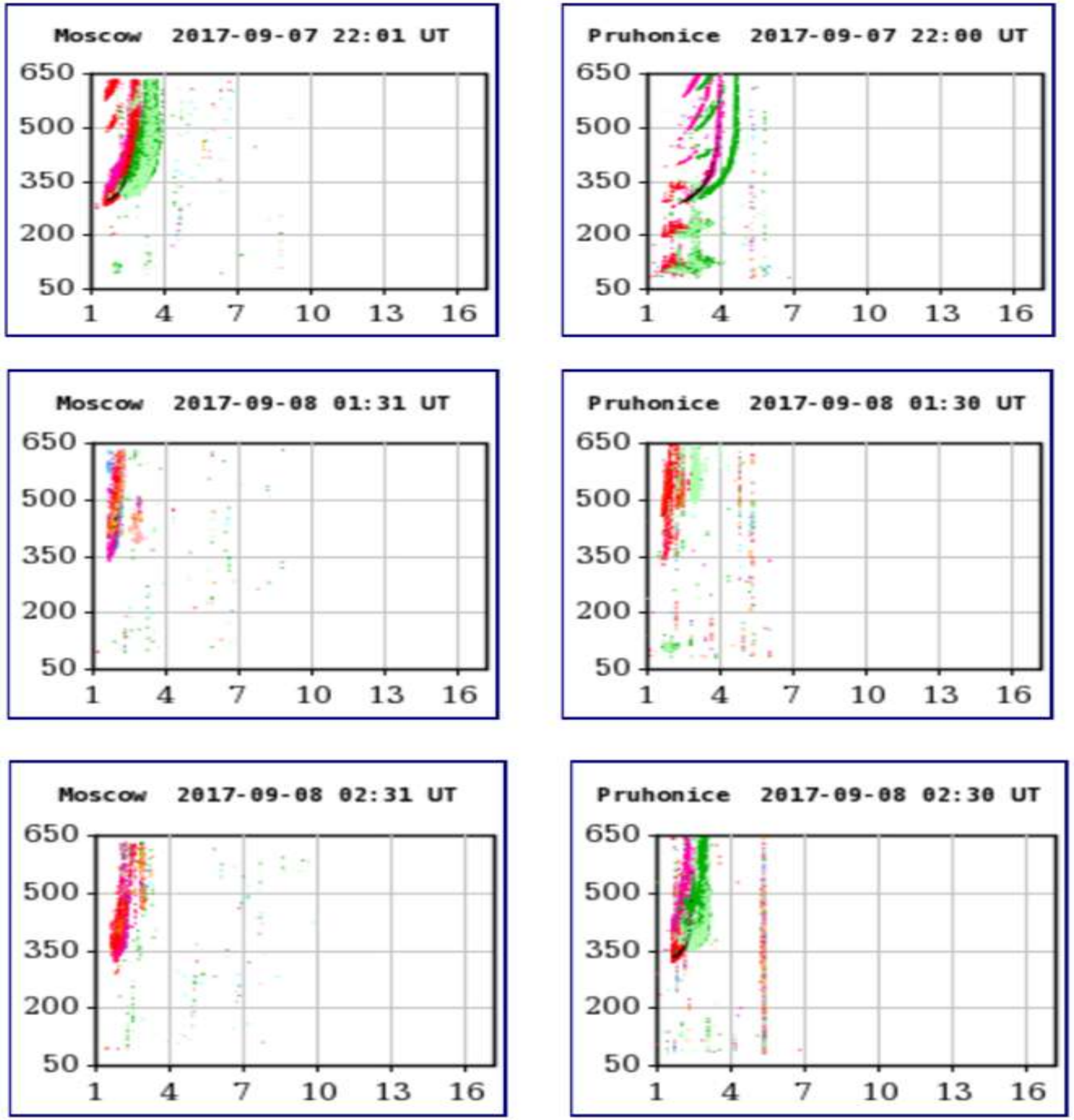

Spread F development over high mid-latitude ionosonde stations during the negative storm

Ionospheric effects of Sep 7-8 2017

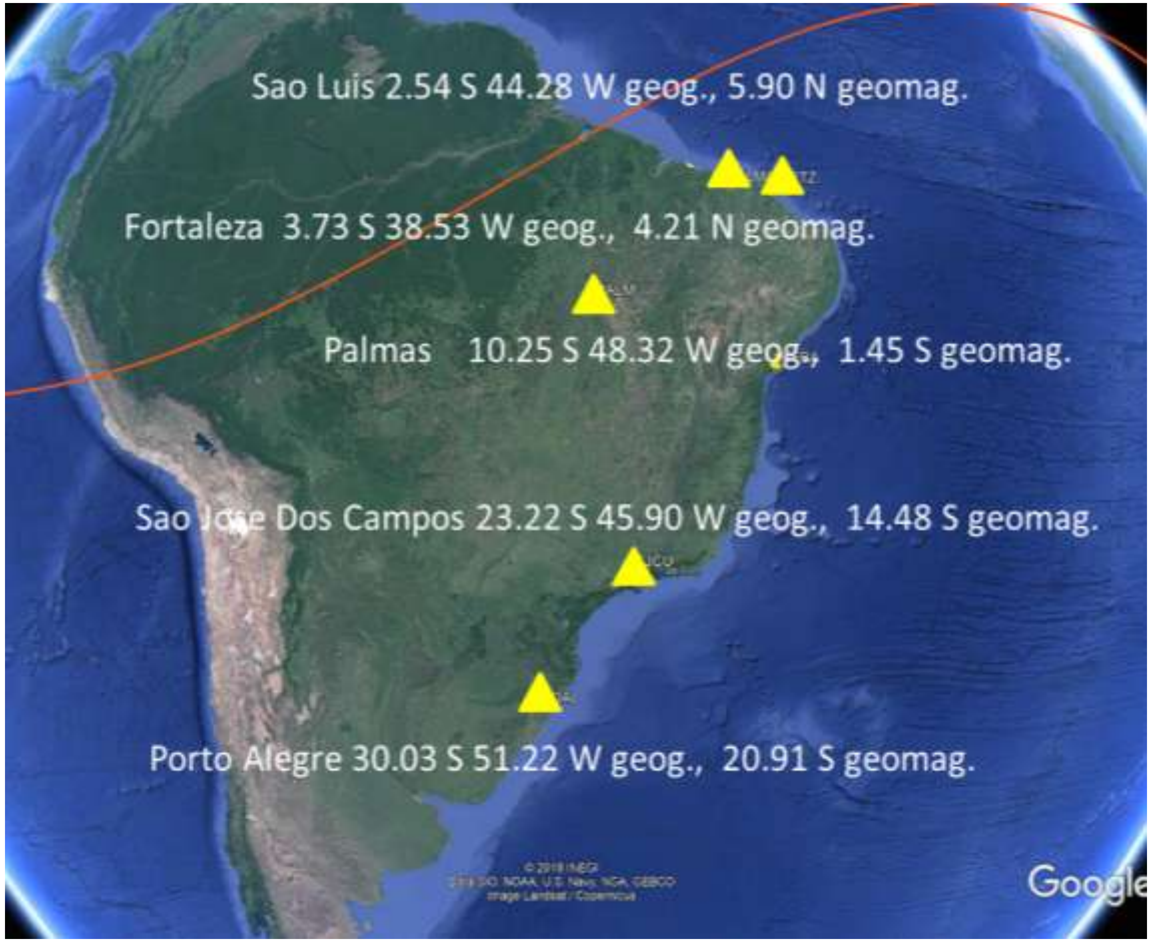

Scintillation events over low- and mid-latitude stations during the negative storm

Data courtesy INGV

Ionospheric effects of Sep 7-8 2017 –Scintillation events in SH

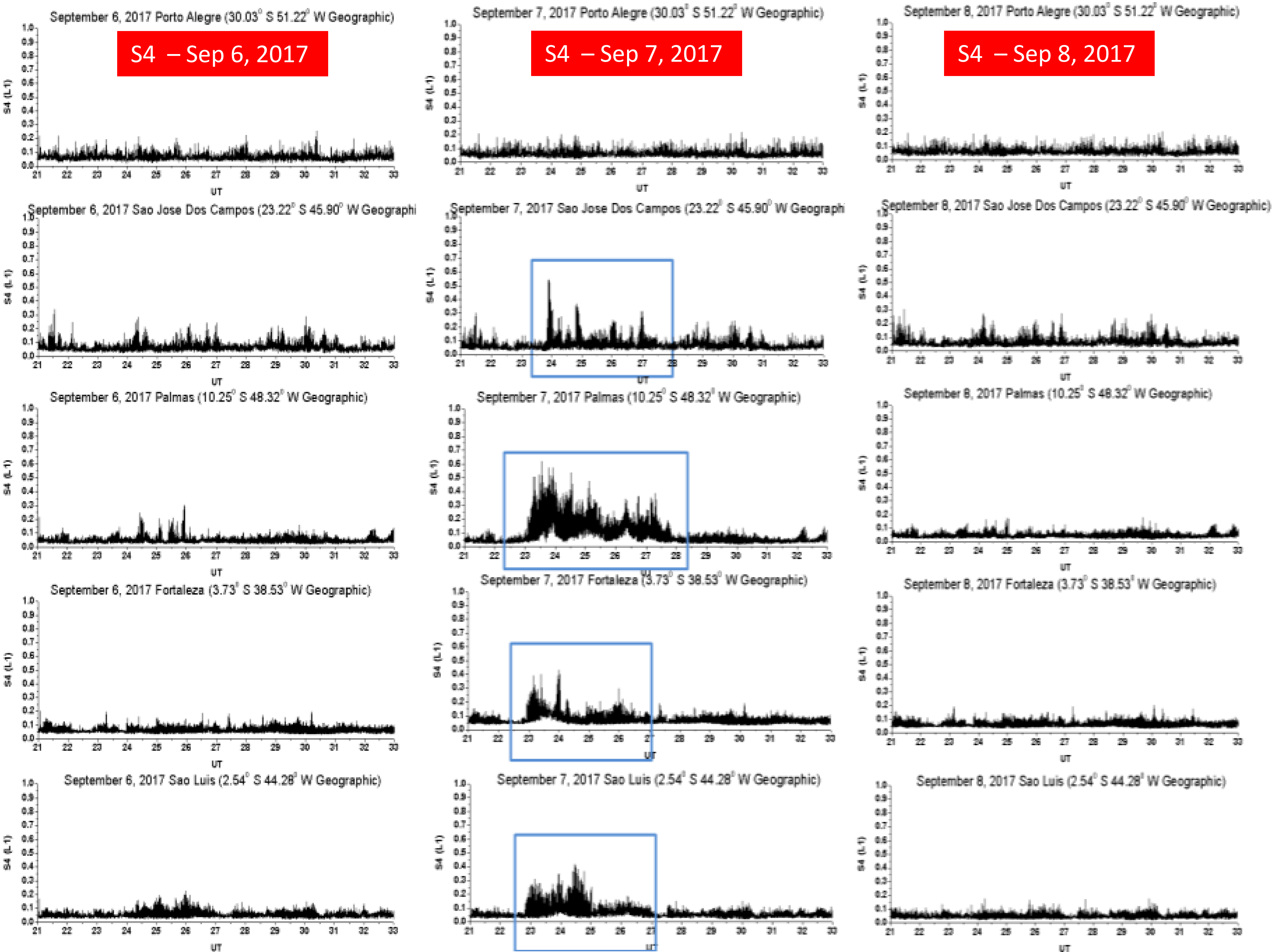

Ionospheric effects of Sep 8 2017 –Scintillation events in SH

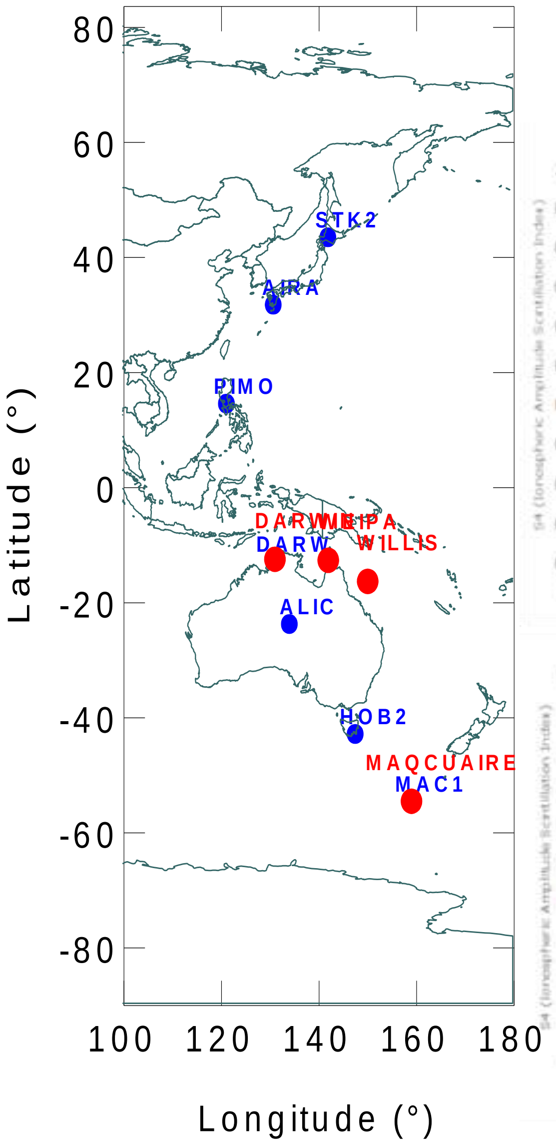

S4 – Sep 8, 2017

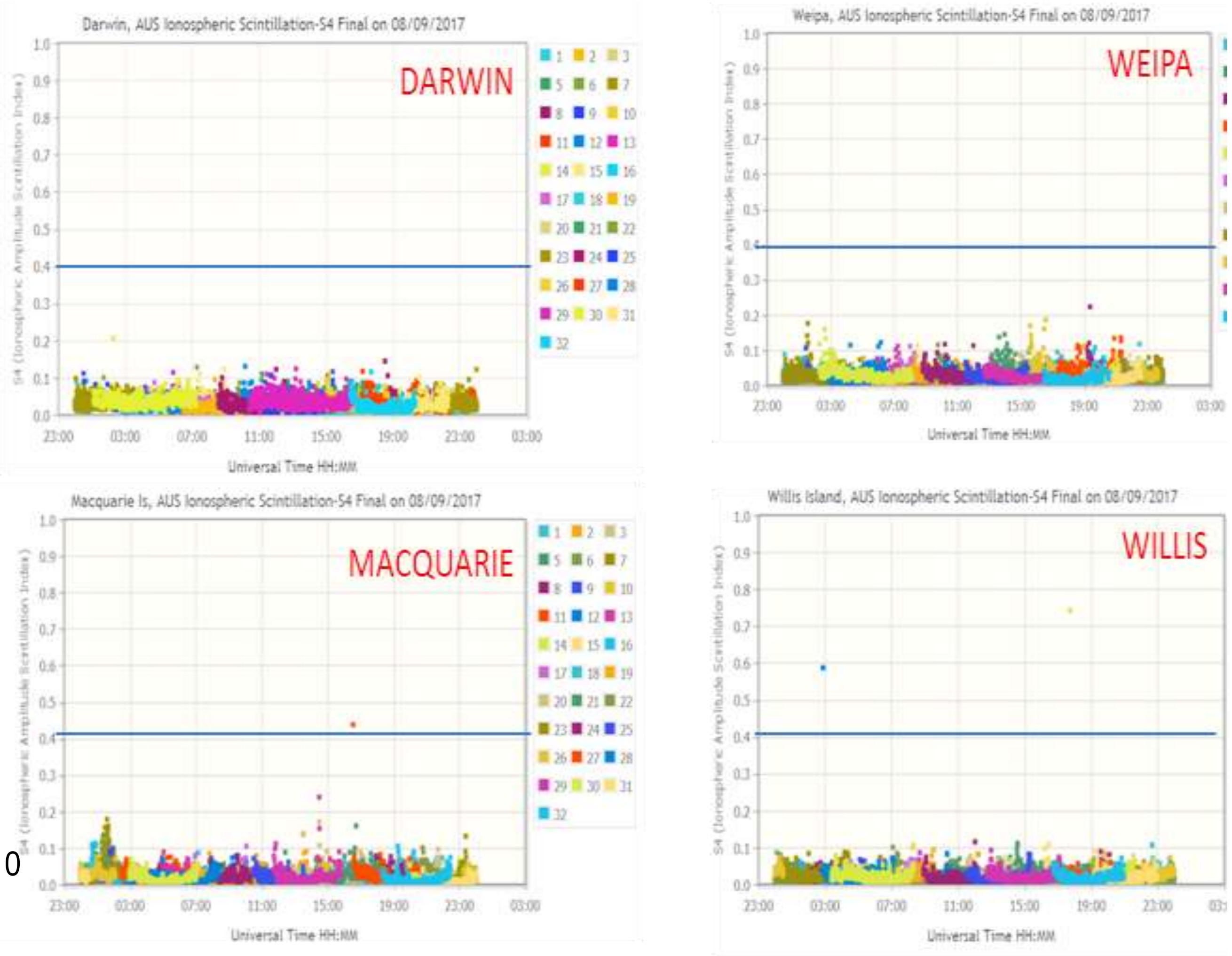

IONOSPHERIC RESPONSE

- Long-lasting, large enhancement of ionospheric TEC in a) all latitudes in Asian sector & in equatorial ,low-latitudes in all sectors but slightly over India – consistent with PROLLS 2nd category

- Long-lasting, large depletion of ionospheric TEC in mid and high-mid latitudes in Europe, India and America sector – consistent with PROLLS 4th category

IONOSPHERIC EFFECTS

- Spread F development during negative storm

- Moderate/low scintillations effects in South Hemisphere regions (S. America & Australia)

Study of Joule Heating and Total Electron Content during Intense Storms of 2015-2017

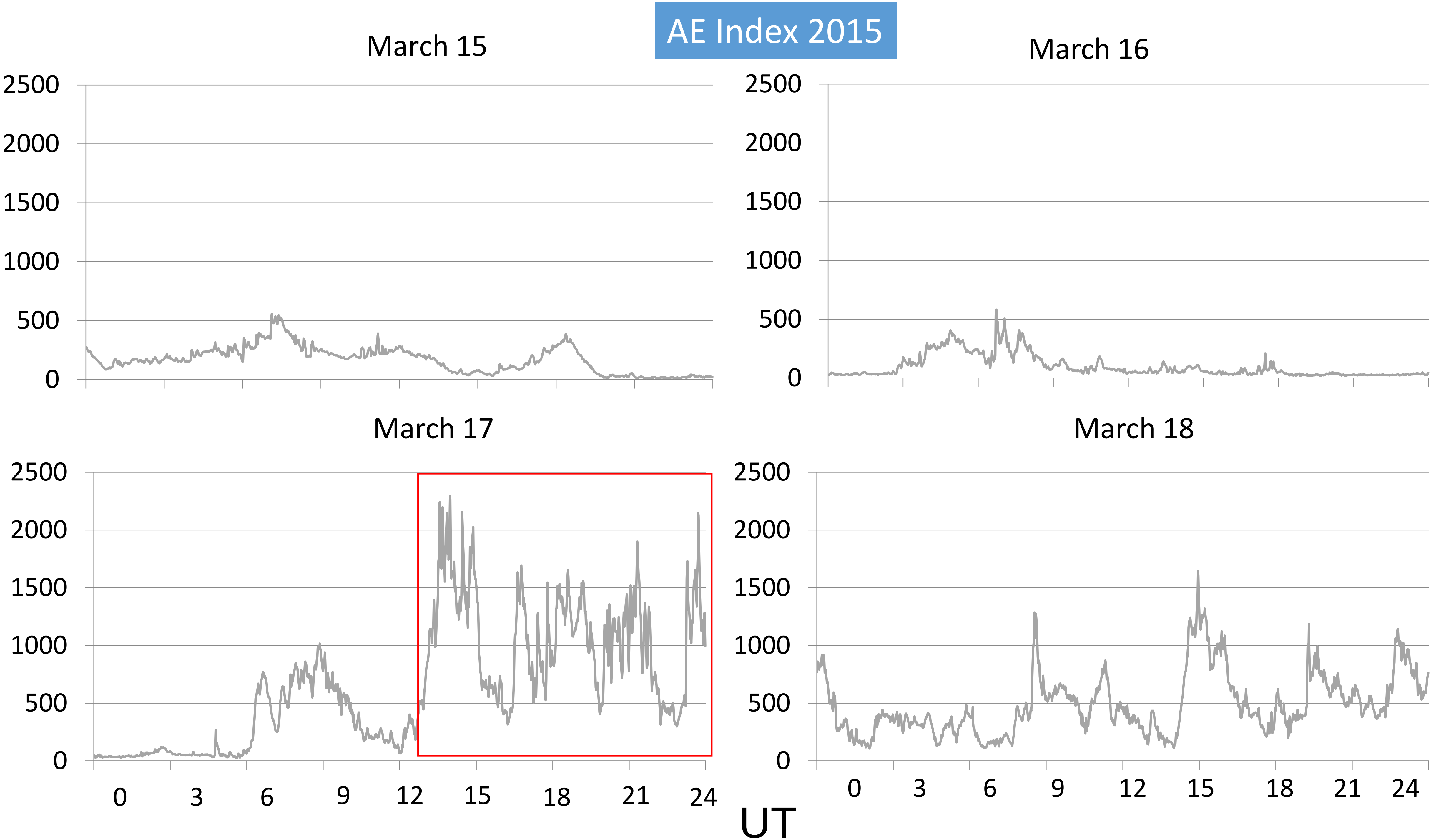
AE Index 2015
March 15
March 16
March 17
March 18
2500
2000
1500
1000
500
0
0
3
6
9
12
15
18
21
24
UT

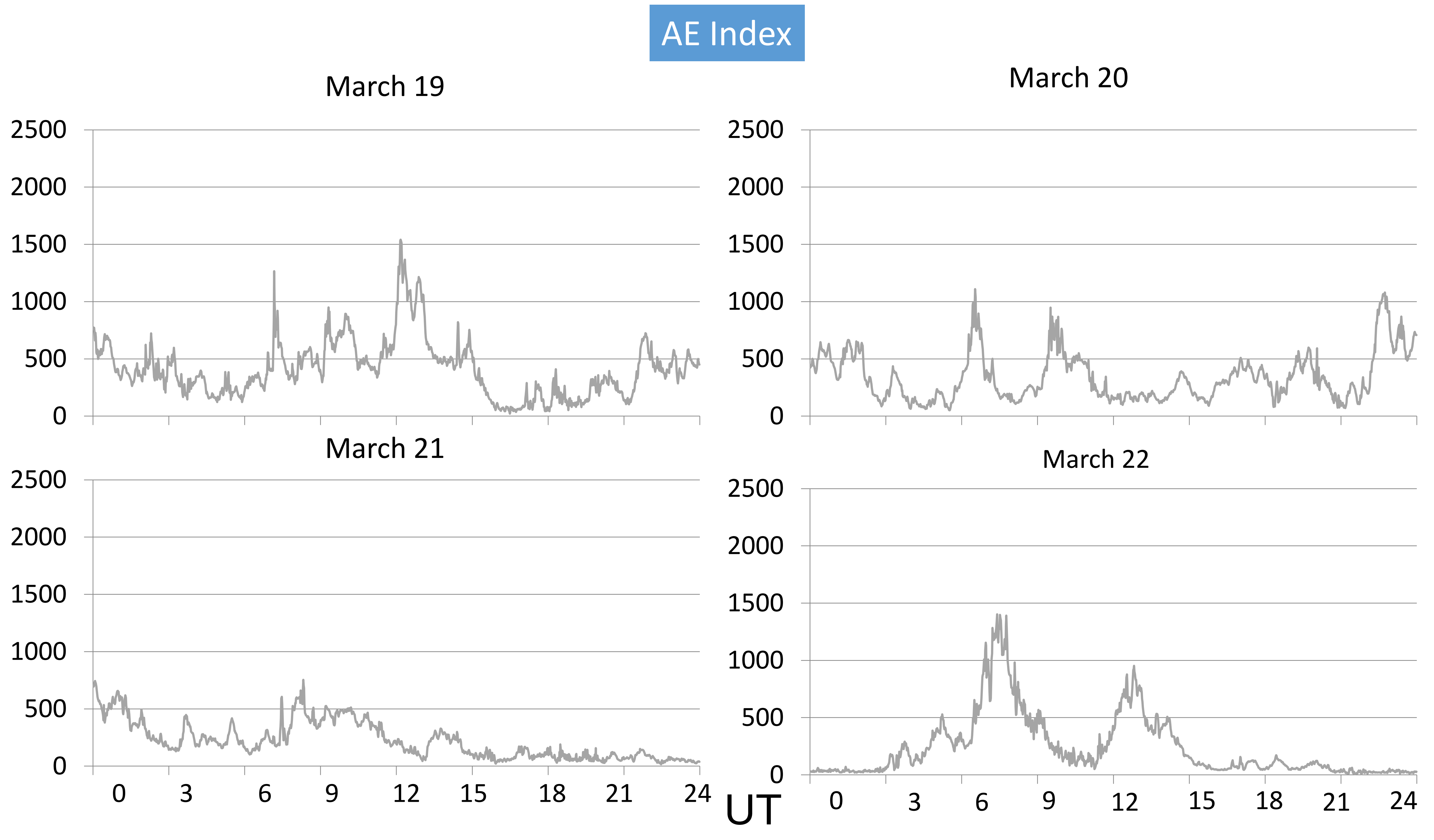
AE Index
March 19
March 20
March 21
March 22
2500
2000
1500
1000
500
0
0
3
6
9
12
15
18
21
24
UT

Thermospheric O/N2 Ratio from GUVI

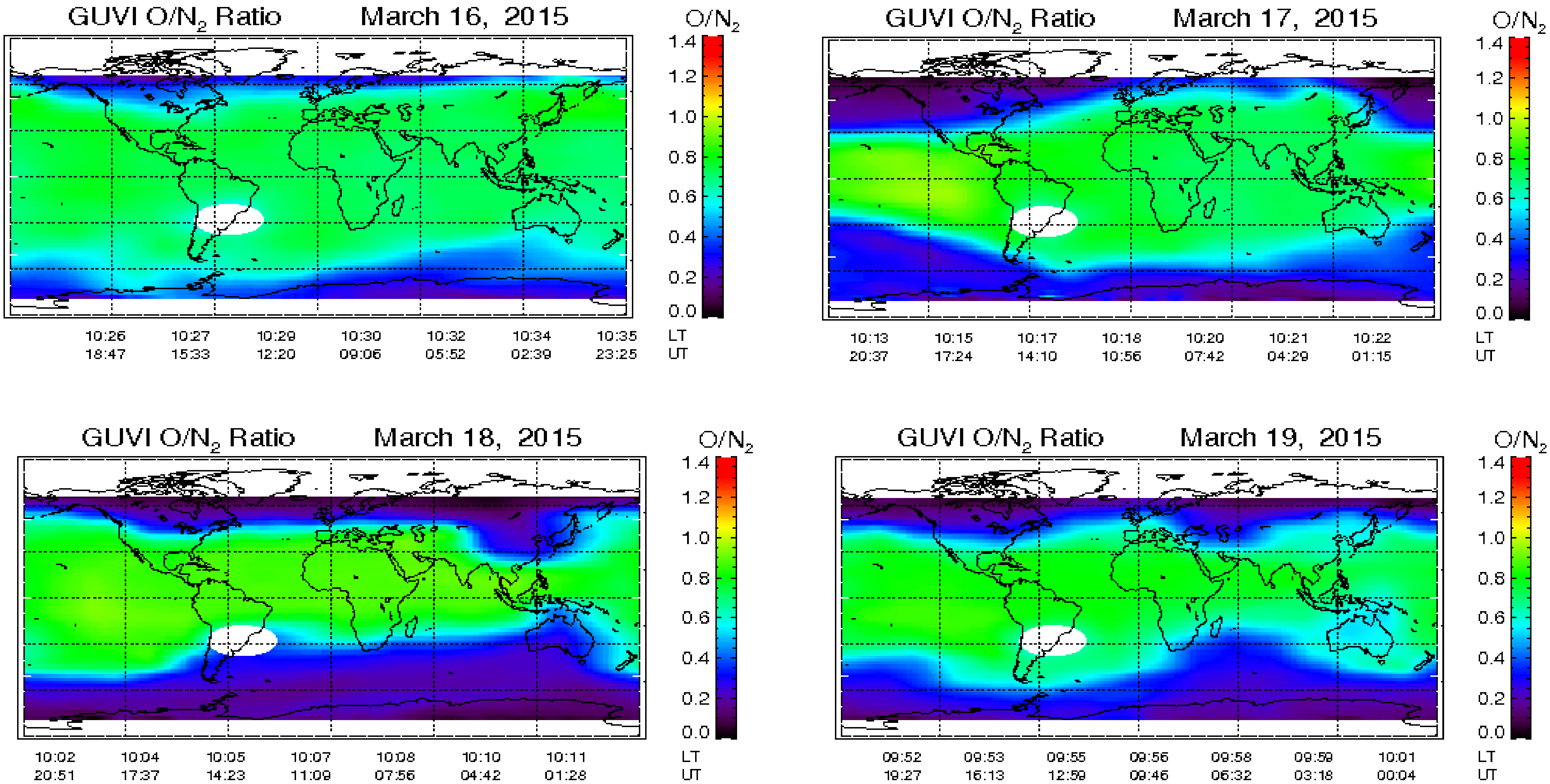

Differential O/N2 ratio (%)

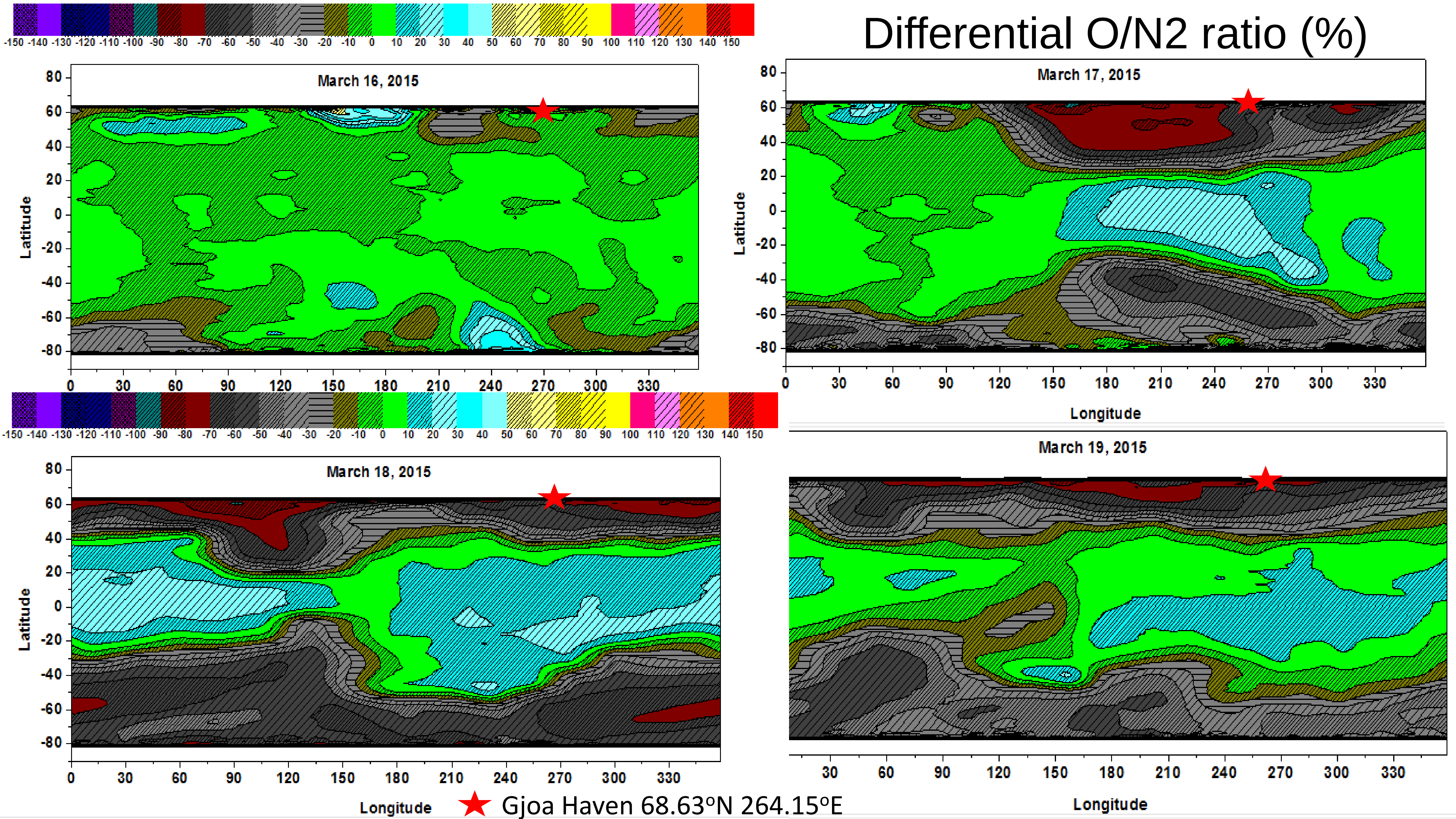

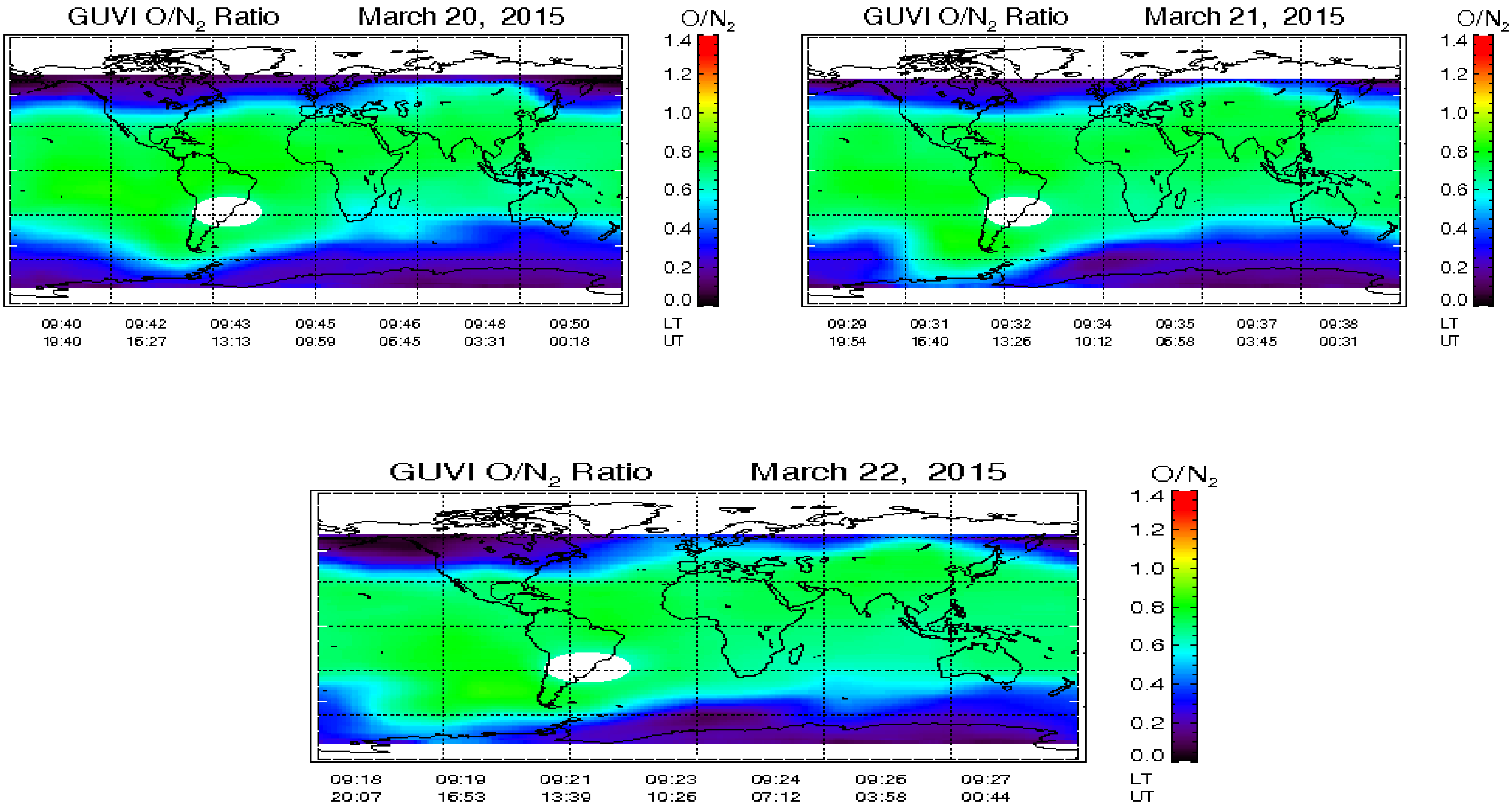
GUVI O/N_2 Ratio March 20, 2015
O/N_2
1.4
1.2
1.0
0.8
0.6
0.4
0.2
0.0
09:40 09:42 09:43 09:45 09:46 09:48 09:50 LT
19:40 16:27 13:13 09:59 06:45 03:31 00:18 UT
GUVI O/N_2 Ratio March 21, 2015
O/N_2
1.4
1.2
1.0
0.8
0.6
0.4
0.2
0.0
09:29 09:31 09:32 09:34 09:35 09:37 09:38 LT
19:54 16:40 13:26 10:12 06:58 03:45 00:31 UT
GUVI O/N_2 Ratio March 22, 2015
O/N_2
1.4
1.2
1.0
0.8
0.6
0.4
0.2
0.0
09:18 09:19 09:21 09:23 09:24 09:26 09:27 LT
20:07 16:53 13:39 10:26 07:12 03:58 00:44 UT

Differential O/N2 ratio

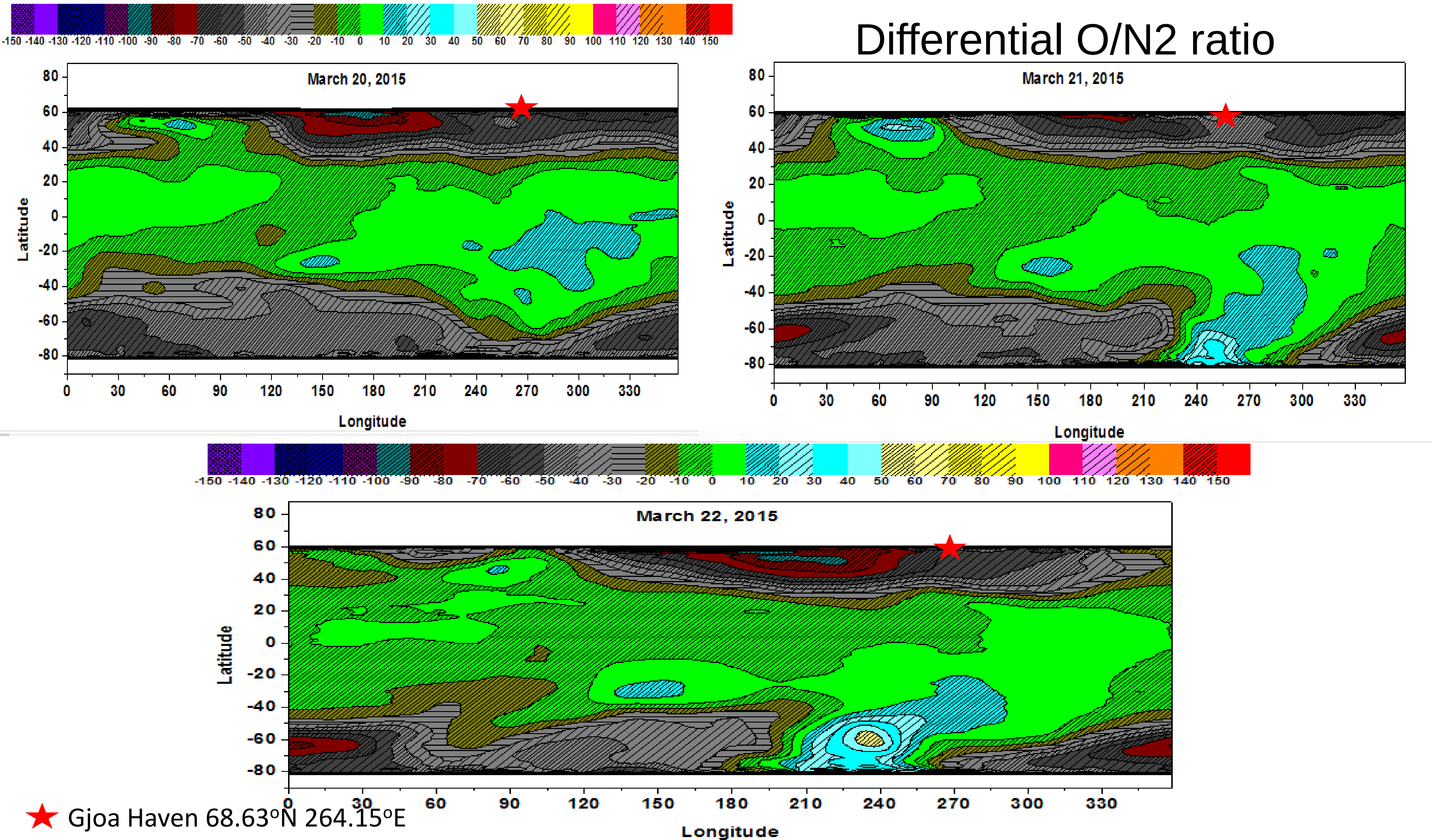

★ Gjoa Haven 68.63°N 264.15°E

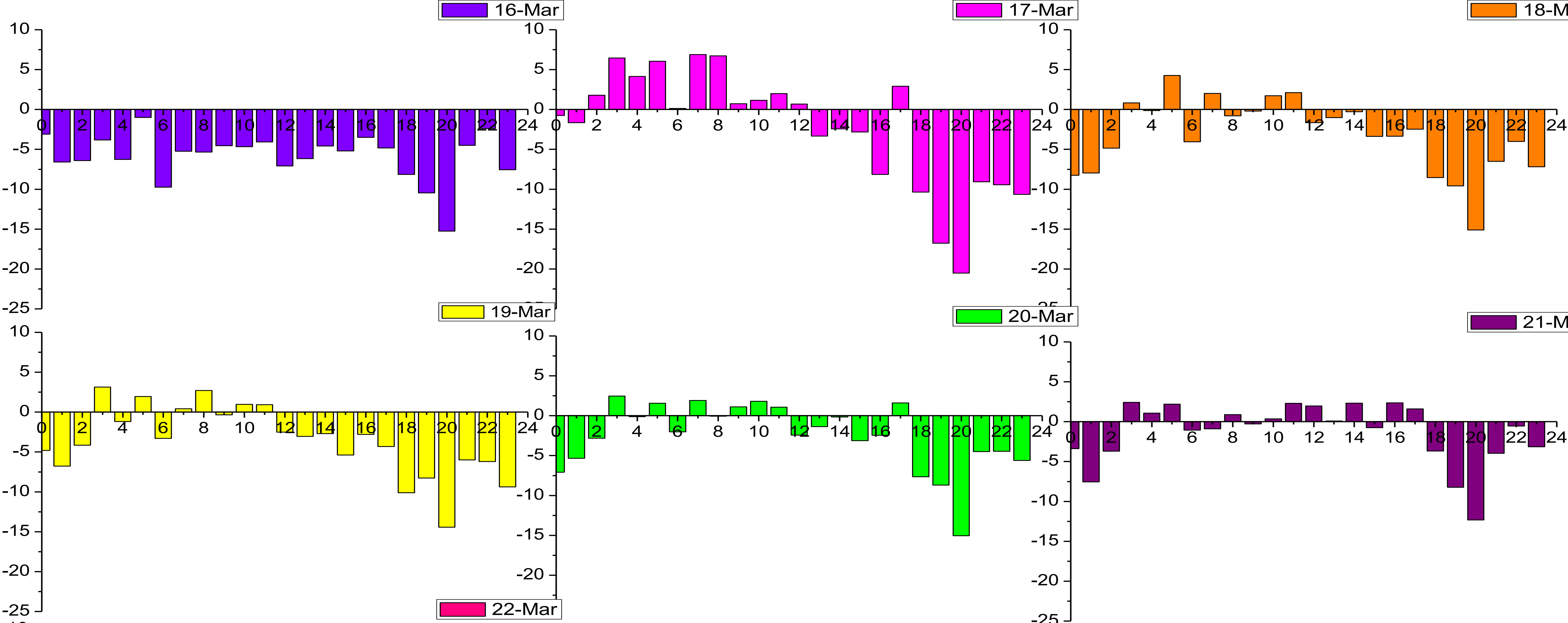

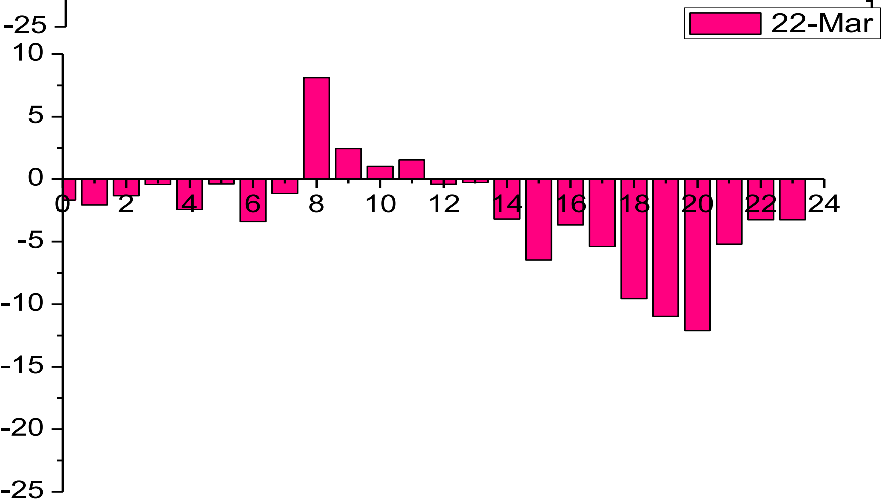

LT = UT – 06.39h

Gjoa Haven 68.63°N 264.15°E

Differential VTEC

Satellite signal outages observed from a network of stations distributed over two hemispheres during periods of scintillations to check conformity with ICAO specified requirements for APV

- The work is conducted preliminarily from Canadian High Arctic Ionospheric Network (CHAIN, Canada) network and CIGALA/CALIBRA (Brazil).

- Specifically at Gjoa Haven and Presidente Prudente

- Currently the same work is conducted from polar regions from stations operated by INGV.

- Specifically at Longyearbean, Mario Zuccheli and Concordia


GJOA HAVEN
Presidente Prudente

No cycle slip found from Canadian CHAIN stations on November 17, 2013.

November 17, 2013

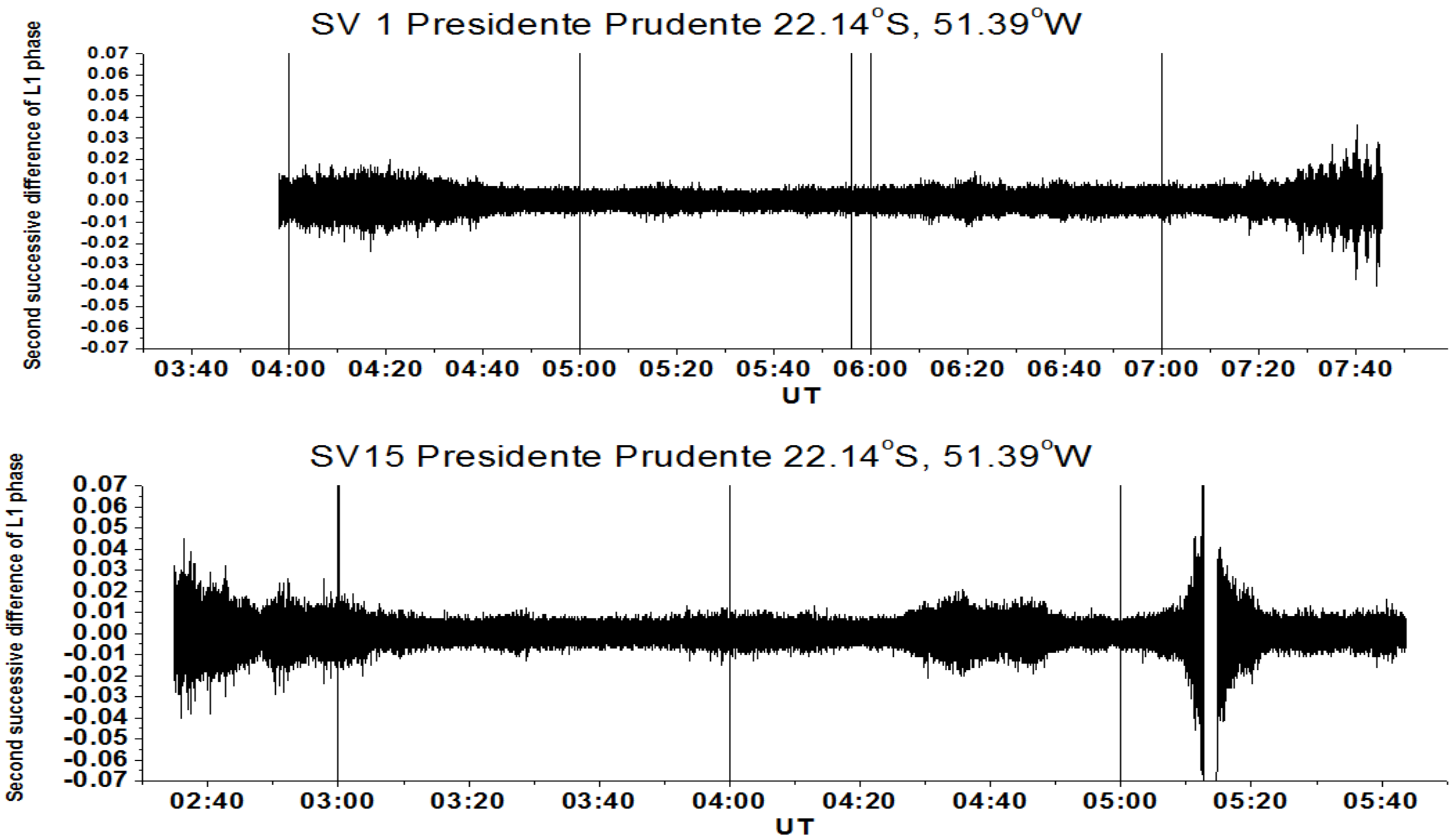

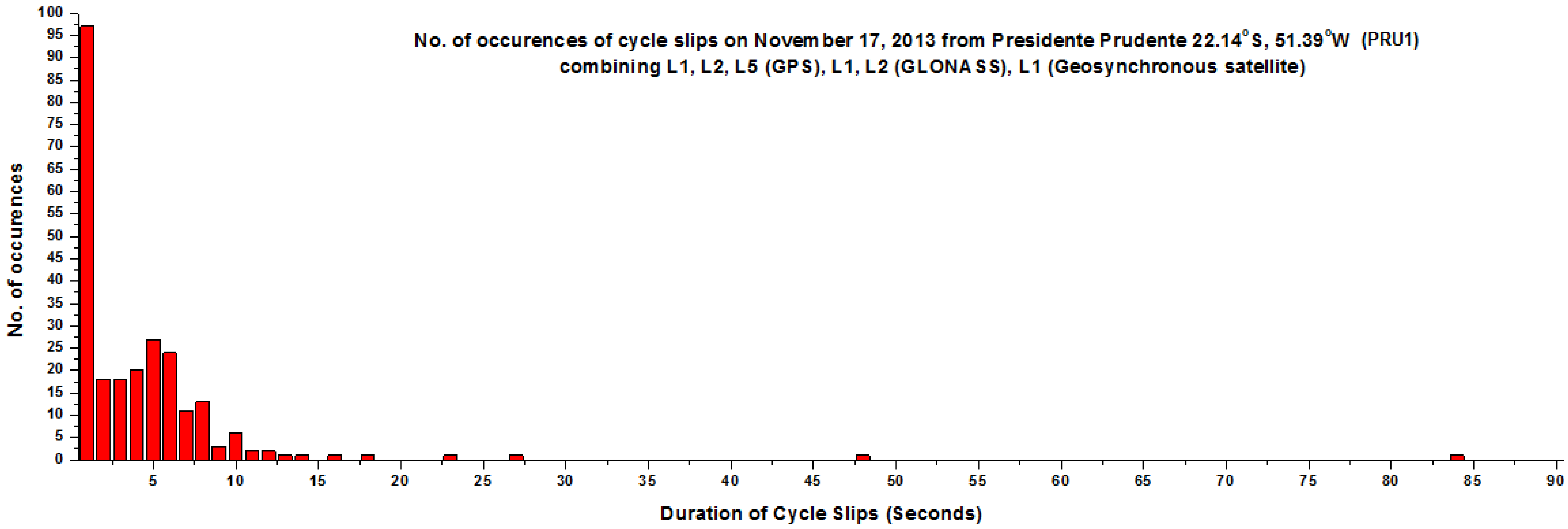

No. of occurences of cycle slips on November 17, 2013 from Presidente Prudente 22.14°S, 51.39°W (PRU1)
combining L1, L2, L5 (GPS), L1, L2 (GLONASS), L1 (Geosynchronous satellite)
No. of occurences
Duration of Cycle Slips (Seconds)

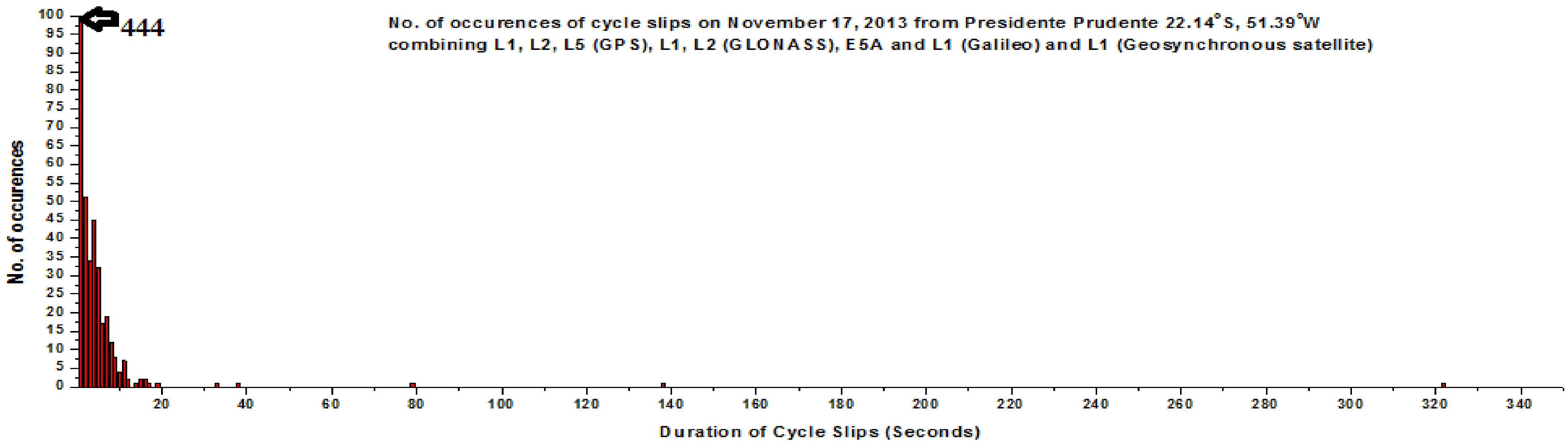

444
No. of occurences of cycle slips on November 17, 2013 from Presidente Prudente 22.14°S, 51.39°W
combining L1, L2, L5 (GPS), L1, L2 (GLONASS), E5A and L1 (Galileo) and L1 (Geosynchronous satellite)
No. of occurences
Duration of Cycle Slips (Seconds)

Polar Stations chosen for measurement of cycle slips

1. Longyearbean LYB 78.2232° N, 15.6267° E geographic, Inclination 82.213 Declination 7.060 as per 21 September, 2012

2. Mario Zucchelli MZS 74.70° S, 164.11° E geographic, Inclination -82.576, Declination 134.636, as per 21 September, 2012

3. Concordia DMC 75.10°S, 123.35°E geographic, Inclination -80.723, Declination -141.236, as per 21 September, 2012

Only geomagnetic quiet days (Dst > -50 nT, kp =< 3 or Ap =< 15) are considered

Geographical Locations of the stations

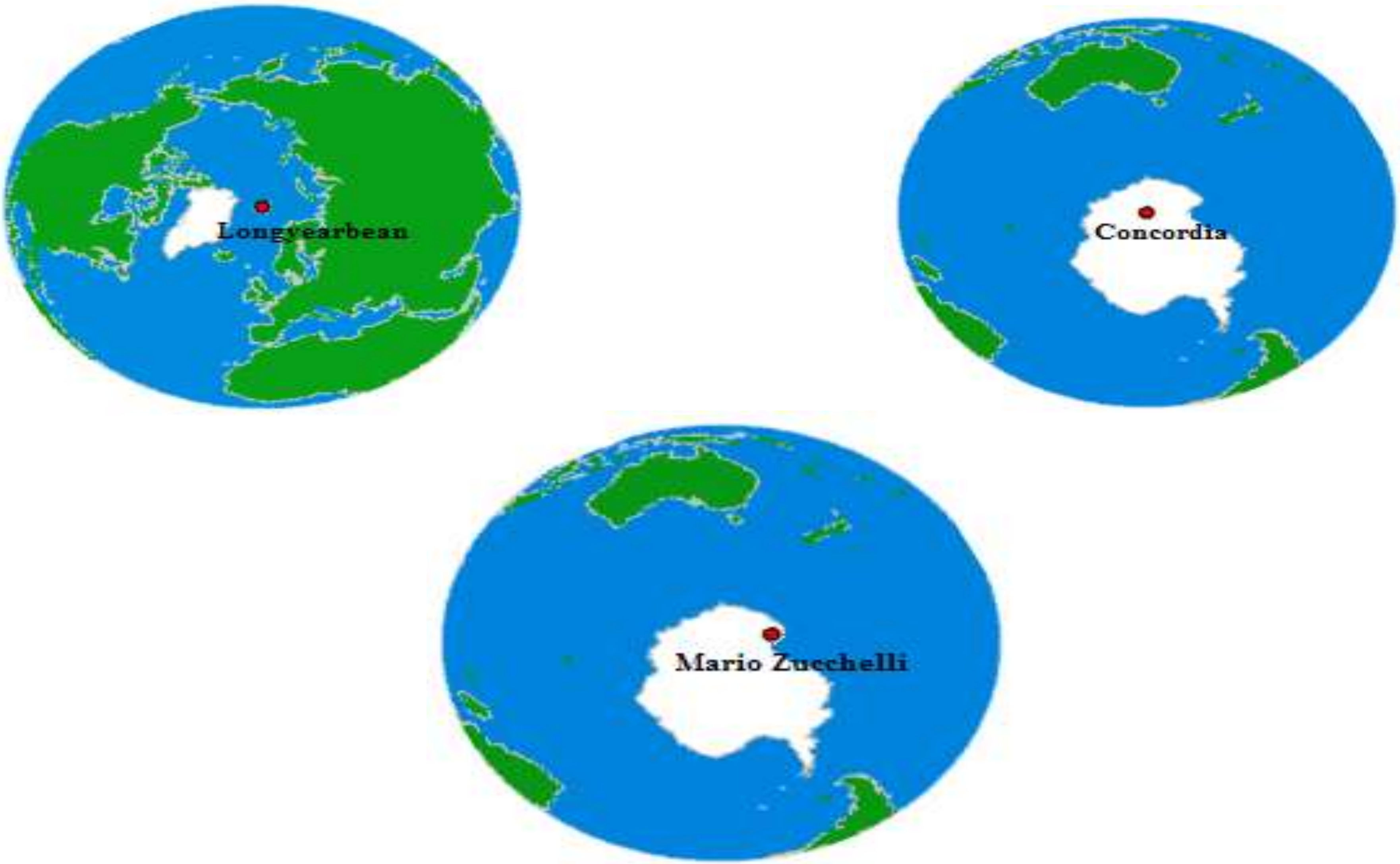

Identify and characterize definitive condition for enhancement or inhibition of scintillation activities corresponding to intense geomagnetic storms for the low latitudes focussing on the geophysically sensitive Indian longitude sector

Siliguri and Calcutta data to look for EIA northern crest scintillations over India

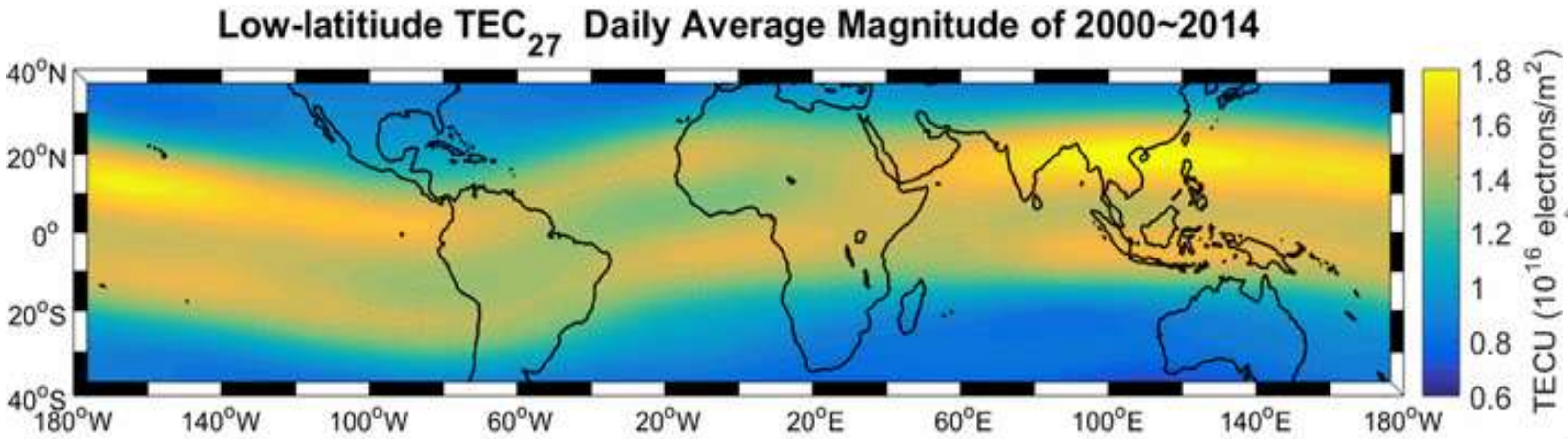

Yao et al. Journal of Geodesy, 2017

Siliguri station

Calcutta station

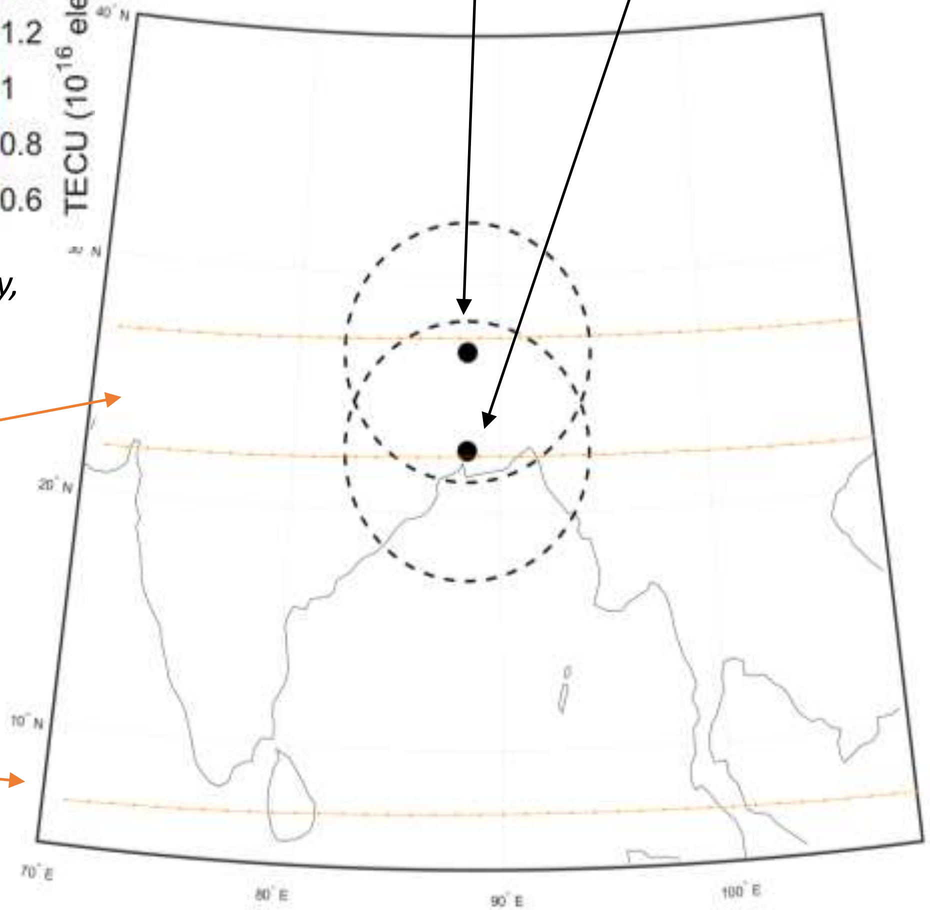

Average position of the crest

Average position of the dip equator

September 2017 storm

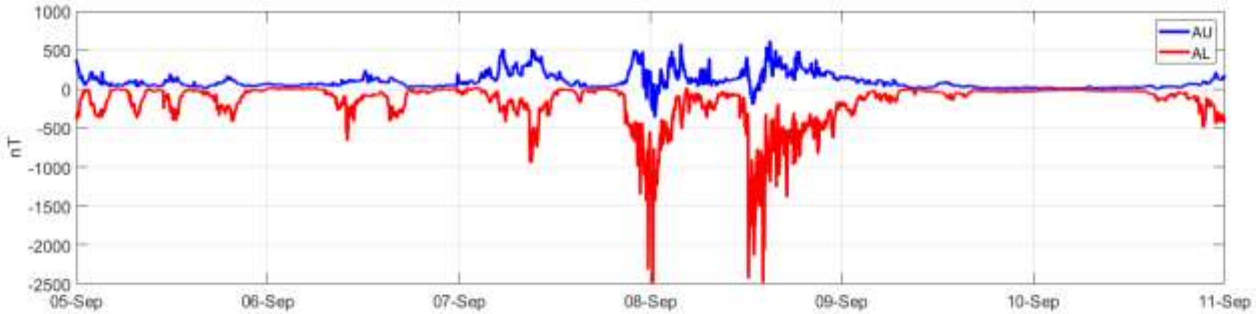

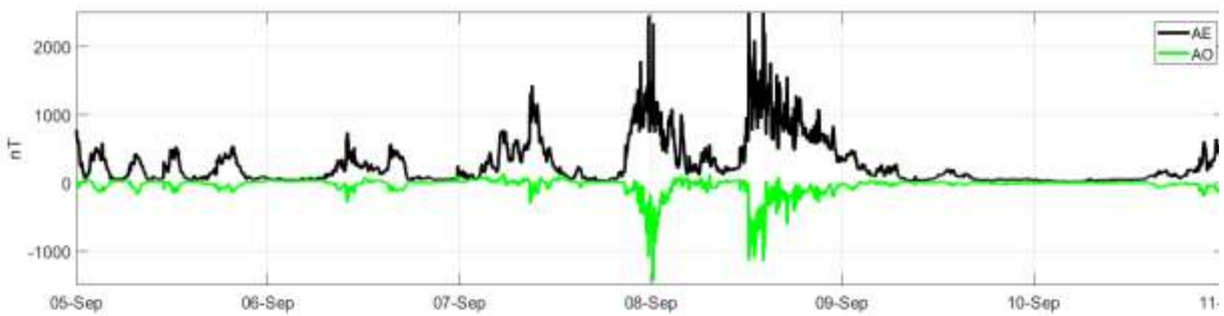

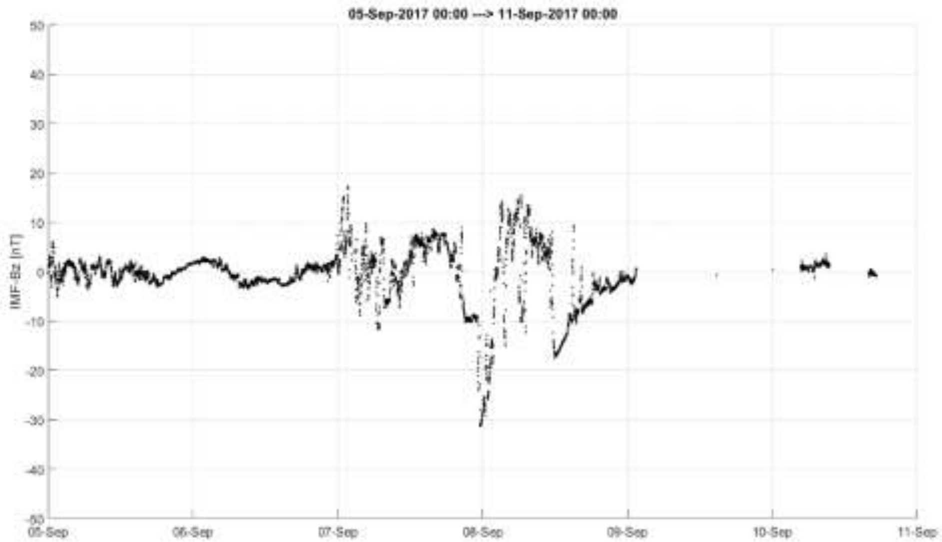

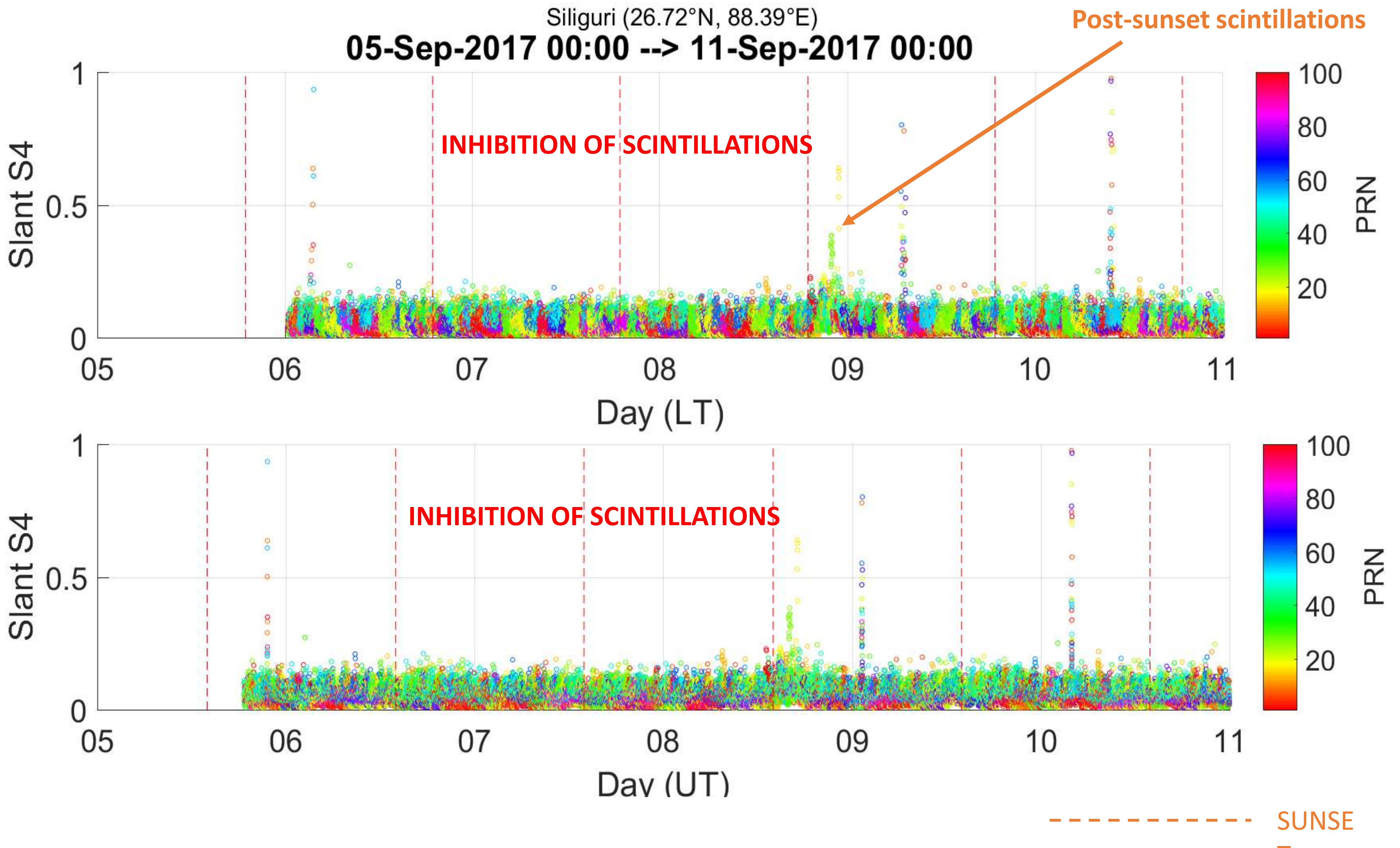

Siliguri (26.72°N, 88.39°E)
05-Sep-2017 00:00 --> 11-Sep-2017 00:00
Post-sunset scintillations
INHIBITION OF SCINTILLATIONS
Slant S4
Day (LT)
PRN
INHIBITION OF SCINTILLATIONS
Slant S4
Day (UT)
PRN
SUNSE

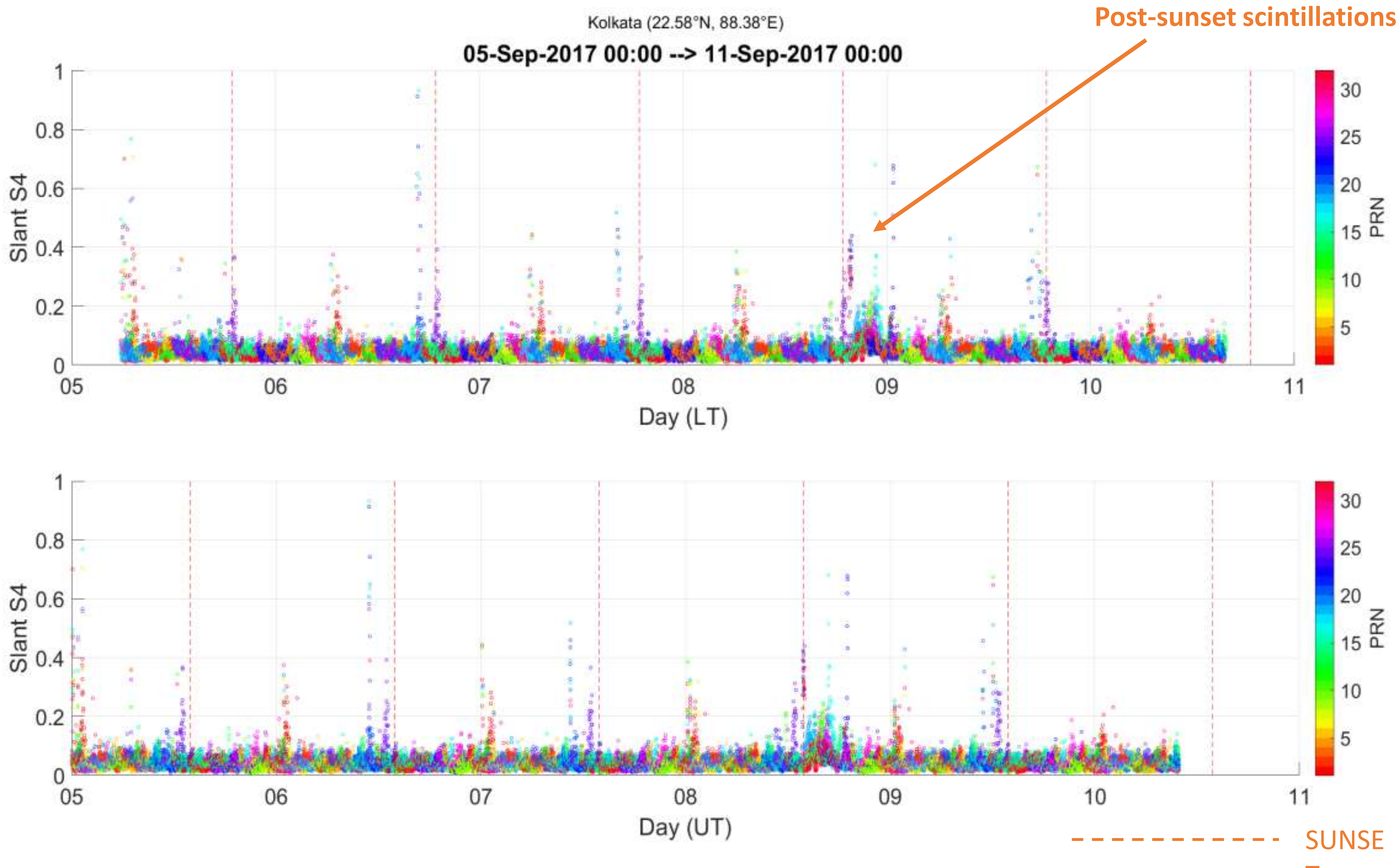
Kolkata (22.58°N, 88.38°E)
05-Sep-2017 00:00 --> 11-Sep-2017 00:00
Post-sunset scintillations
Slant S4
Day (LT)
PRN
Slant S4
Day (UT)
PRN
SUNSE

FINAL AIM: CLIMATOLOGY OF IONOSPHERIC SCINTILLATIONS OVER INDIA

An example from the CIGALA/CALIBRA GNSS network in Brazil from 2013 to 2015

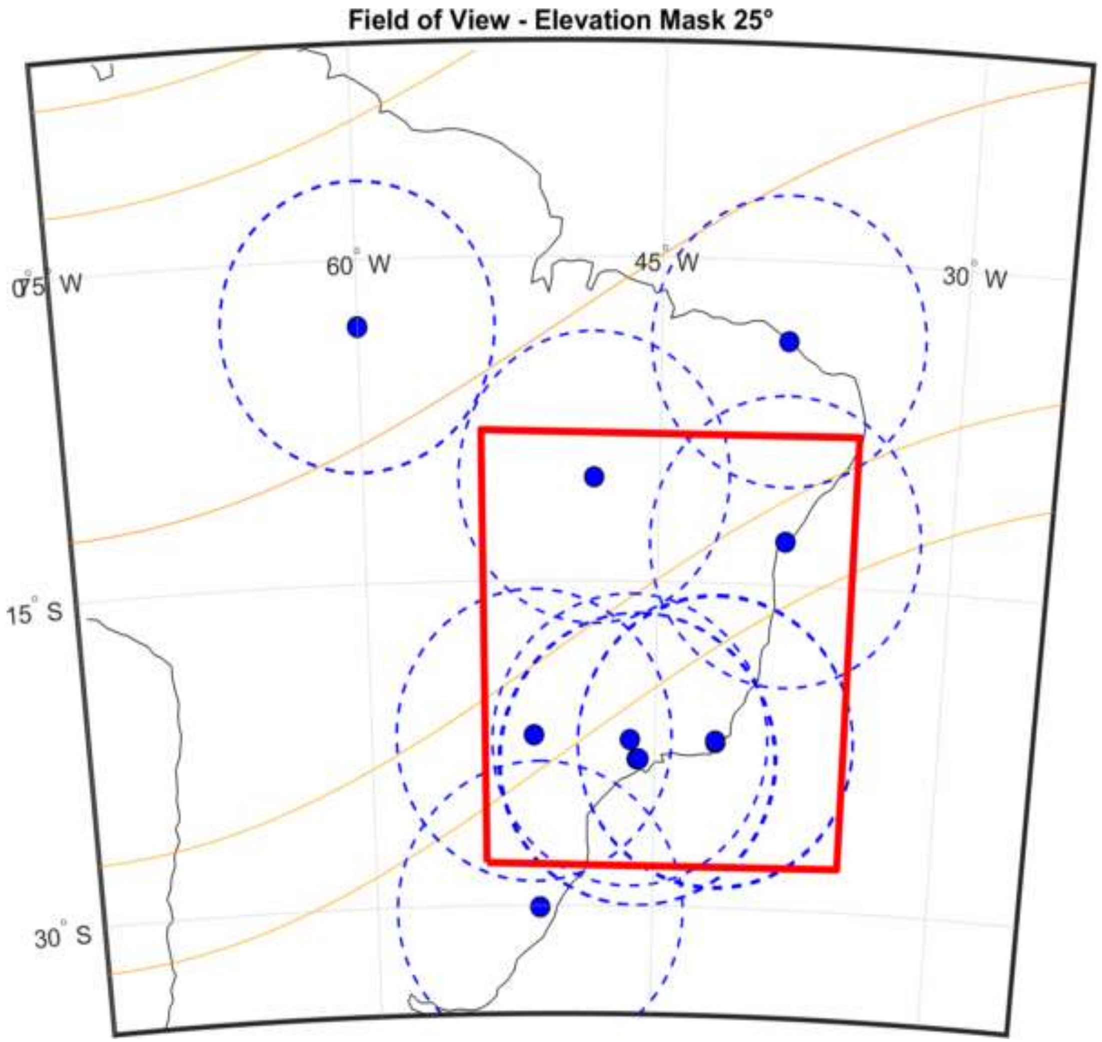

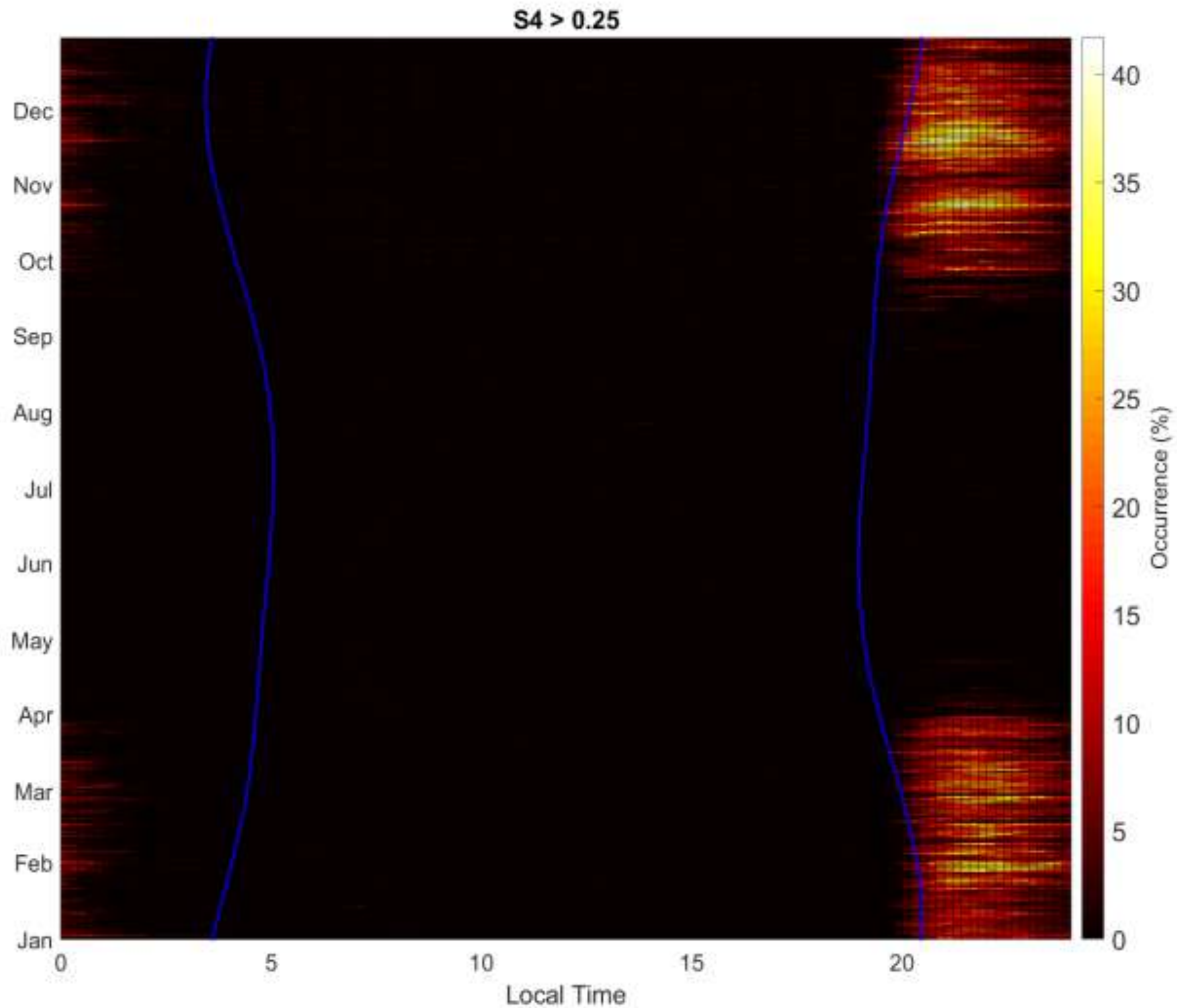

SERB, DST Sponsored ST Radar Project at the Ionosphere Field Station, Haringhata of the University of Calcutta

Principal Investigator: Prof. Ashik Paul
Co-Principal Investigator: Dr. J. Y. Siddiqui

Co-Investigator: Mr. Souvik Majumdar

Stratosphere Troposphere Radar Facility at University of Calcutta Ionosphere Field Station, Haringhata

The ST (Stratosphere Troposphere) Radar has proved to be a useful and versatile tool for lower atmospheric and ionospheric studies. Appreciating that the lower atmosphere is the seat of many interesting physical phenomena with implications to global change, University of Calcutta is implementing Eastern and North-Eastern India's first ST Radar at 53MHz at the Ionosphere Field Station, Haringhata located about 50 km north-east of the city.

Objectives

i. To study the dynamics of the tropopause and Stratosphere Troposphere Exchange (STE)
ii. To study the convection process in troposphere
iii. To characterize rain structure based on radar signatures of precipitating layers
iv. To study lower atmospheric turbulence
v. To study gravity waves and planetary scale waves and their effects on the upper atmosphere
vi. To study ionospheric E and F region irregularities

Configuration

ST Radar is fully active phased array radar, operating at 53MHz. Its planar antenna array consists of 475 numbers of three-element Yagi antennas each fed by a dedicated 2-kW Solid-state coherent Transmit-Receive (TR) Module. The array is configured in a near-circular shape spreading over an area of about 7000m². An inter-element spacing of 0.7λ is adopted with an equilateral triangular grid to steer the beam up to a zenith angle of 30°. Antenna array is organized into 25 sub-array groups each consisting of 19 Yagi elements.

Performance Parameters:

Height coverage: 0.5 - 20 km, with useful observations over at least 90% of time under all atmospheric conditions.
Height resolution: 50 m up to 3 km altitude, 150 m from 3 to 20 km altitude
Horizontal wind velocity: 1 - 70 m/s
Vertical wind velocity: 0.1 - 30 m/s
Velocity resolution: Better than 1% of maximum velocity value
Wind accuracy: Horizontal wind speed 1 m/s, direction 10
Time resolution: 5-15 min for full profile
Average power aperture product at the antenna feed point: 3.0x10⁸wm² or better

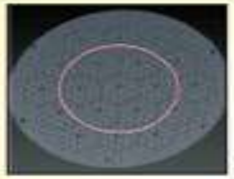

475 elements
25 subarrays
53MHz operating frequency with 3MHz BW
Peak Power of 2KW per TR Module

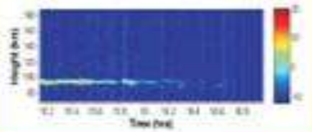

Deliverables:

1. Three component wind measurements provide information about wave disturbances; 2. Spectral width measurements contain information on microscale turbulence; 3. The reflectivity measurements contain information on small scale turbulence as well as large scale temperature gradients associated with tropopause; 4. The most important and unique capability of the ST radars is the measurement of the vertical wind componentwith a high degree of temporal and altitude resolutions (typically ~ 30sec and ~ 150m). This unique capability gives the ST radars an enormous advantage over the conventional wind measurement techniques.

LOW MODE
37.5-m resolution
7 sub arrays (133 Elements)
133-kW Power
0.25-us uncoded pulse
Height coverage : 5km

HIGH MODE
75-150 m resolution
ALL sub arrays (475 Elements)
950-kW Power
coded pulse
Height coverage 20km

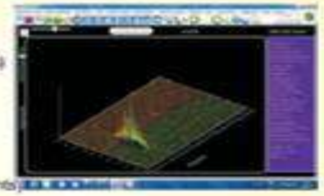

Funded by Science and Engineering Research Board (SERB), DST, GoI

- Fully Active Phased Array Radar, operating at 53 MHz with a bandwidth of 3MHz.
- Planar antenna array with 475 three-element Yagi antennas
- Beam Steering up to an off-zenith angle of 30^o
- Organized into 25 sub-array groups each with 19 Yagi antenna elements and a shelter for housing TRMs

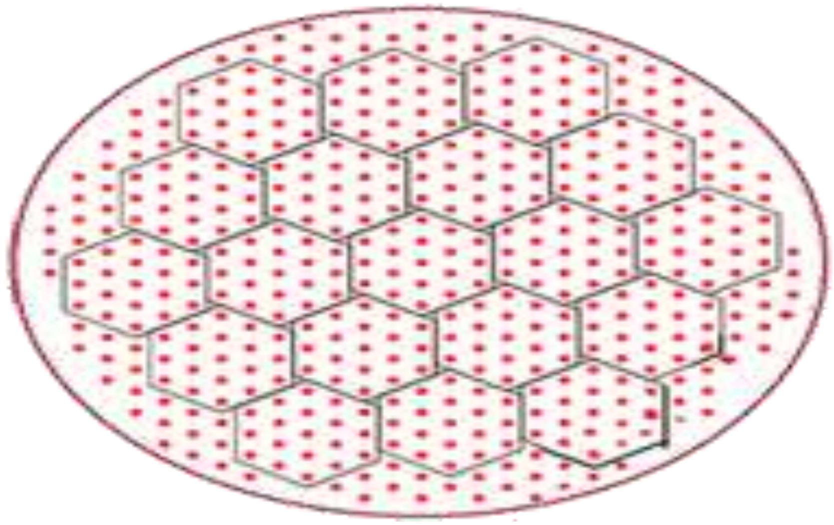

ST RADAR ARRAY
With Near-Circular Shape

Performance Parameters	
Height coverage	0.5-20km for 90% of time
Height resolution	i) 50m up to 3km ii) 150m from 3-20km
Horizontal wind velocity	1-70m/s
Vertical wind velocity	0.1-30m/s
Time resolution	5-15min for full profile
Average power aperture product	3×10^8 Wm^2

Original digital receiver design had 18 channels. But now it is being upgraded to 25 channels

ST Radar Pilot Array (19-Element)

Control & Instrumentation Room

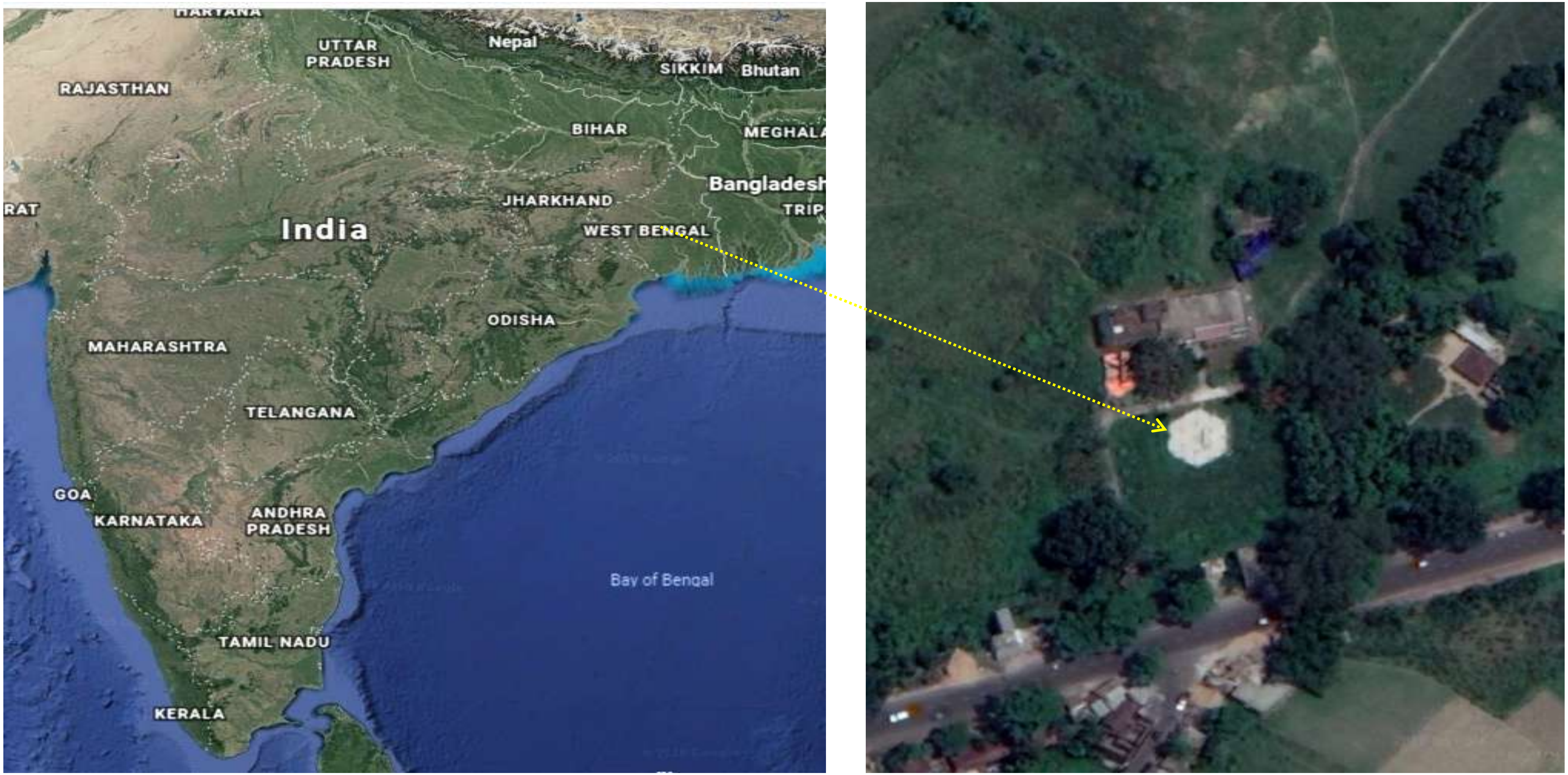

ST Radar Pilot Array, Ionosphere Field Station, Haringhata
University of Calcutta (22.93 N, 88.50 E Geo)

- Pilot Array operational at Haringhata since April 2018


Tropical Cyclone Phailin
8 PM EDT Thu Oct 10 2013
Position 15.8 N 88.8 E
Maximum Winds 155 mph
Gusts 190 mph
Movement WNW at 6 mph
Blue Marble basemap imagery courtesy NASA
Satellite 5:27 AM UTC
1:27 AM EDT

Near Real-Time RO Coverage

UCAR
UNIVERSITY CORPORATION FOR ATMOSPHERIC RESEARCH

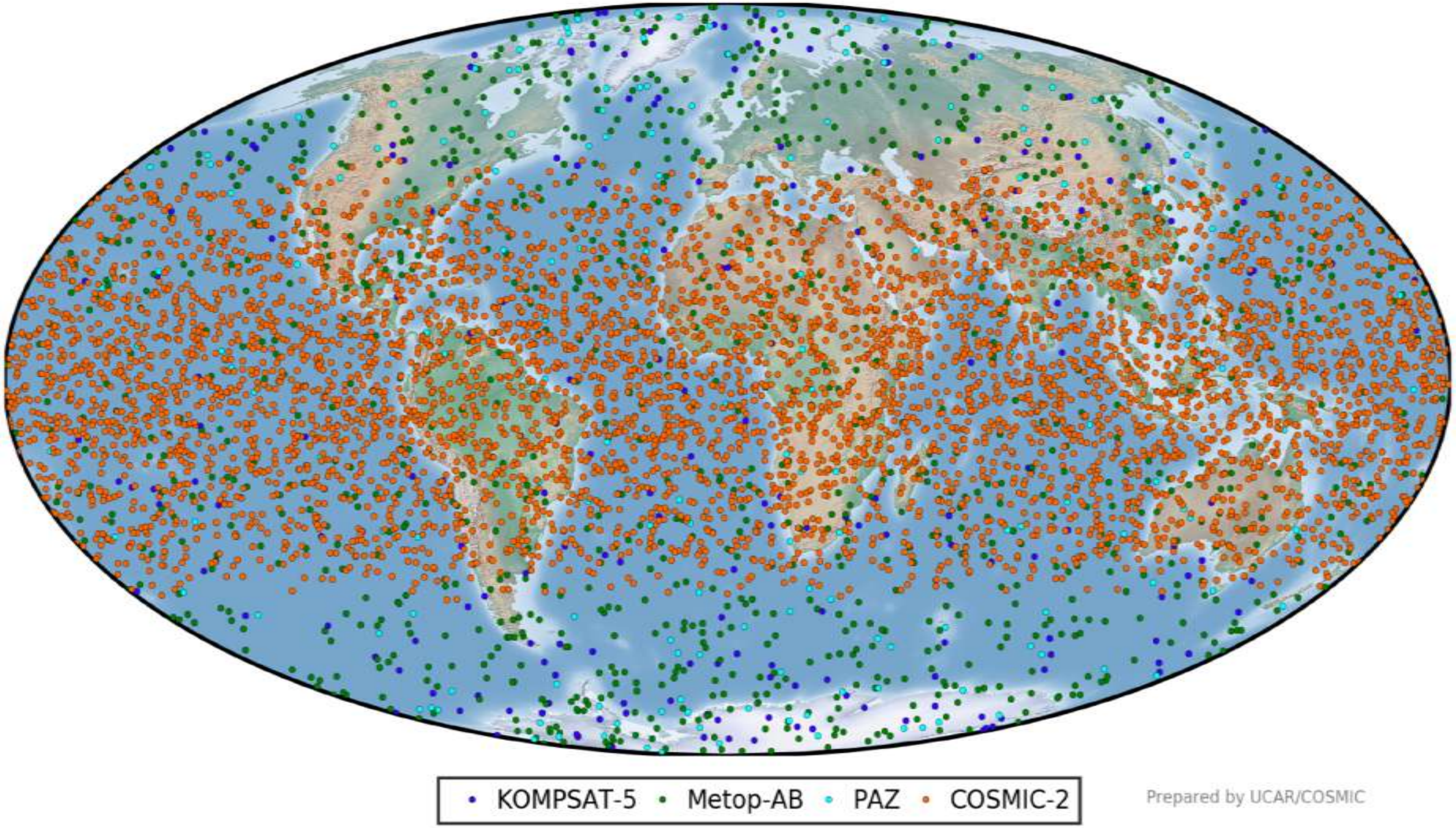

Prepared by UCAR/COSMIC

Scientific Uses of RO Data

- Ionosphere and Space Weather
  - Observe global electronic density distribution
  - Improve the analysis and prediction of space weather
  - Improve monitoring/prediction of scintillation (e.g. equatorial plasma bubbles, sporadic E clouds)

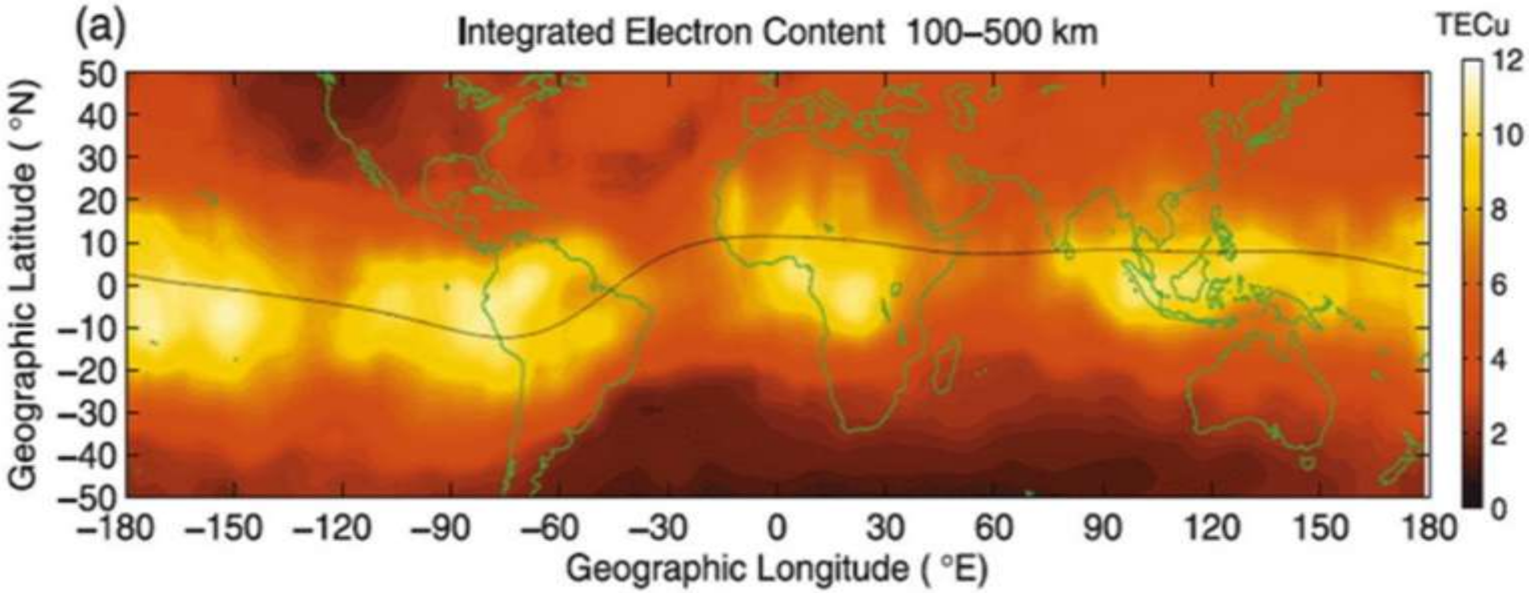

Lin et al, Geophys. Res. Lett., 2007

GNSS Receiver Network

- Motivation
  - Collection of navigation data message bits needed for radio occultation retrievals
  - Support GNSS precise orbit and clock determination
  - Support GNSS science research (free and open data policy)
- Deploying network of GNSS sites
  - ~15 sites
  - Multi-GNSS, triple frequency, geodetic quality
- Approach
  - Core network of UCAR maintained sites
    - We know hardware, firmware, data transmission paths and protocols
    - Aiming for redundant tracking globally to ensure robust coverage
  - Contributed sites
    - Data streams contributed by partner agencies, best effort basis

GNSS Ground Network

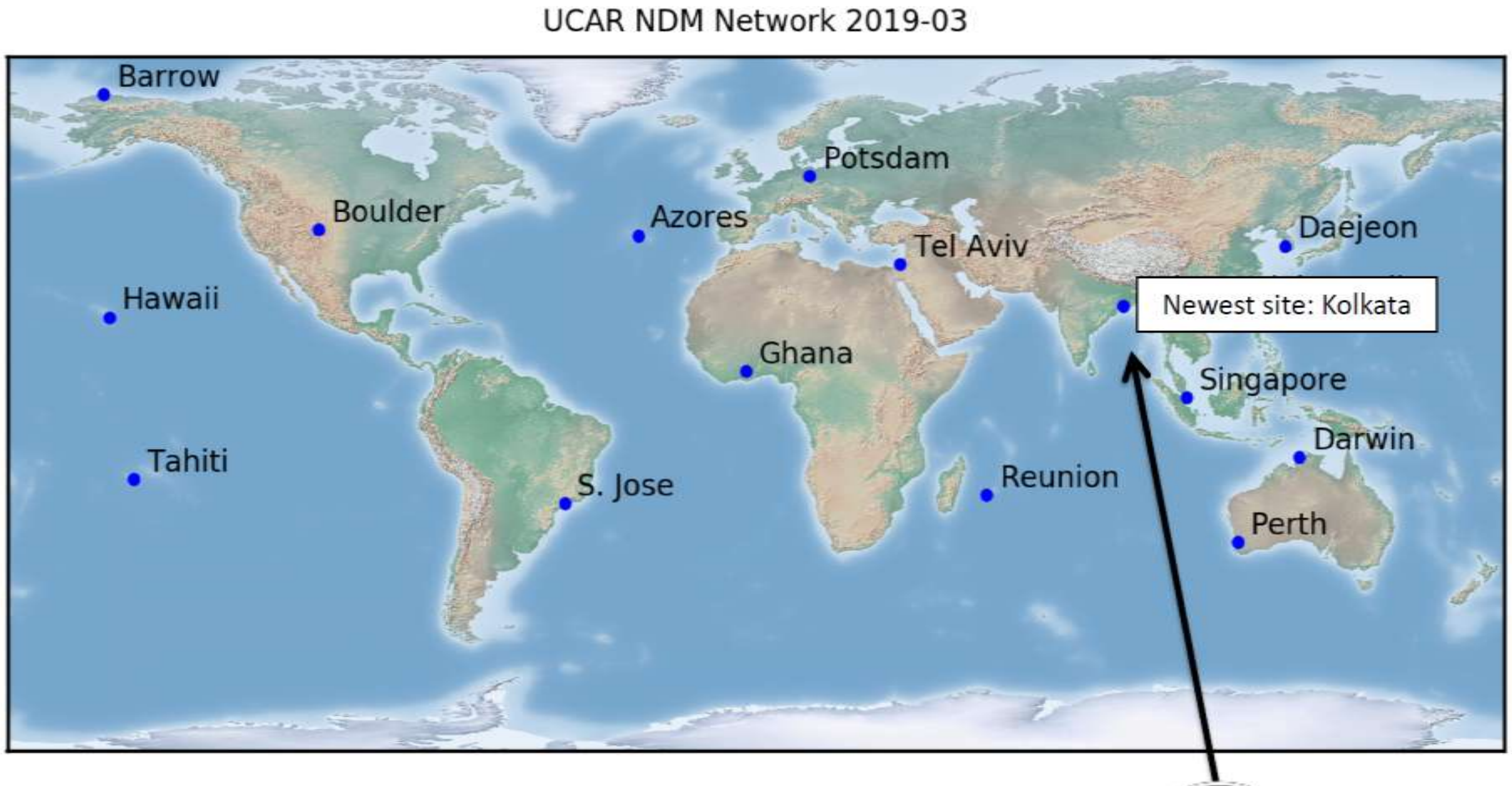

- 2019 additions
  - La Reunion
  - Kolkata

ASHISH KUMAR DASGUPTA
1942-2019

Multi-technique Characterization of Near-Earth Space Environment

Search

ISSI Team led by Prof. Ashik Paul, Institute of Radio Physics and Electronics, University of Calcutta, Calcutta, India

INTERNATIONAL SPACE SCIENCE INSTITUTE

International Team

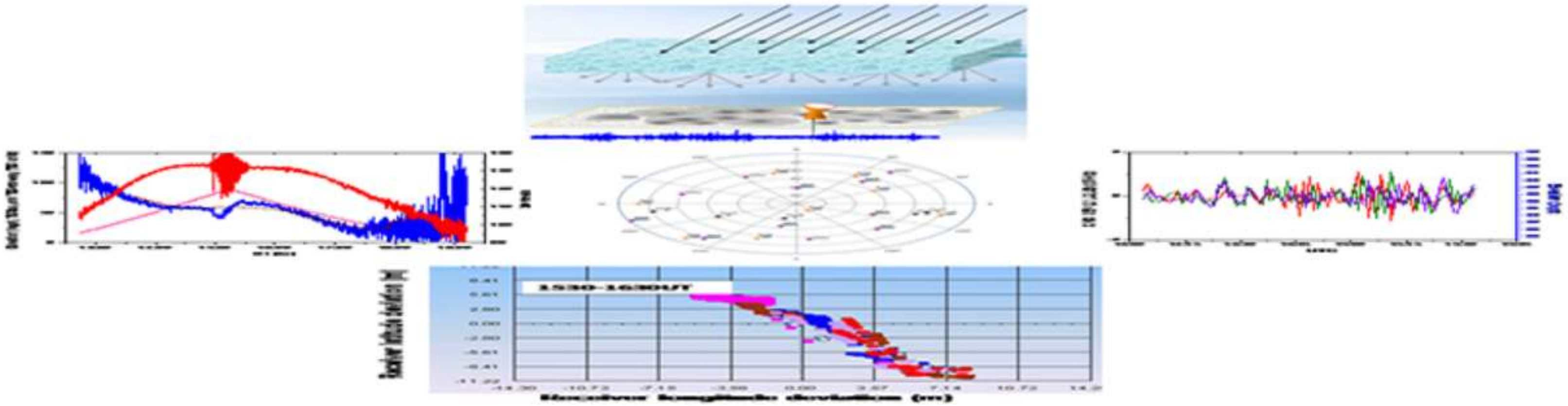

THANK YOU